Carbon loss from northern circumpolar permafrost soils amplified by rhizosphere priming

Authors:

Frida Keuper[1,2,*,†], Birgit Wild[3,4,5,*,†], Matti Kummu[6], Christian Beer[3,4,7,8], Gesche Blume-Werry[2,9], Sébastien Fontaine[10], Konstantin Gavazov[2,11], Norman Gentsch[12], Georg Guggenberger[12,13], Gustaf Hugelius[4,14], Mika Jalava[6], Charles Koven[15], Eveline J. Krab[2,16], Peter Kuhry[4,14], Sylvain Monteux[2], Andreas Richter[17,18], Tanvir Shahzad[19], James T. Weedon[20], Ellen Dorrepaal[2]

Affiliations:

[1]BioEcoAgro Joint Research Unit, INRAE, F-02000, Barenton-Bugny, France

[2]Climate Impacts Research Centre, Department of Ecology and Environmental Science, Umeå University, Abisko, Sweden

[3]Department of Environmental Science, Stockholm University, Stockholm, Sweden

[4]Bolin Centre for Climate Research, Stockholm University, Stockholm, Sweden,

[5]Department of Earth Sciences, University of Gothenburg, Gothenburg, Sweden

[6]Water and Development Research Group, Aalto University, Espoo, Finland

[7]Institute of Soil Science, Department of Earth Sciences, Universität Hamburg, Hamburg, Germany

[8]Center for Earth System Research and Sustainability, Universität Hamburg, Hamburg, Germany

[9]Experimental Plant Ecology, Institute of Botany & Landscape Ecology, Greifswald University, Greifswald, Germany

[10]French National Research Institute for Agriculture, Food and the Environment, INRAE, VetAgro Sup, UMR Ecosystème Prairial, Clermont Ferrand, France

[11]Swiss Federal Institute for Forest, Snow and Landscape Research WSL, Lausanne, Switzerland

[12]Institute of Soil Science, Leibniz Universität Hannover, Hannover, Germany

[13]VN Sukachev Institute of Forest, SB-RAS, Krasnoyarsk, Russian Federation

[14]Department of Physical Geography, Stockholm University, Stockholm, Sweden

[15]Climate and Ecosystem Sciences Division, Lawrence Berkeley National Laboratory, Berkeley, CA, USA

[16]Department of Soil and Environment, Swedish University of Agricultural Sciences, Uppsala, Sweden

[17]Centre for Microbiology and Environmental Systems Science, University of Vienna, Vienna, Austria

[18] International Institute for Applied Systems Analysis, Laxenburg Austria

[19]Department of Environmental Sciences & Engineering, Government University College Faisalabad, Faisalabad, Pakistan

[20]Systems Ecology, Department of Ecological Sciences, Vrije Universiteit Amsterdam, Amsterdam, The Netherlands

*Corresponding authors: frida.keuper@inrae.fr; birgit.wild@aces.su.se

[†]The authors contributed equally to this work.

As global temperatures continue to rise, a key uncertainty of climate projections is the microbial decomposition of vast organic carbon stocks in thawing permafrost soils. Decomposition rates can accelerate up to four-fold in the presence of plant roots and this mechanism – termed the rhizosphere priming effect – may be especially relevant to thawing permafrost soils as rising temperatures also stimulate plant productivity in the Arctic. However, priming is currently not explicitly included in any model projections of future carbon losses from the permafrost area. Here we combine high-resolution spatial and depth-resolved datasets of key plant and permafrost properties with empirical relations of priming effects from living plants on microbial respiration. We show that rhizosphere priming amplifies overall soil respiration in permafrost-affected ecosystems by ~12 %, which translates to a priming-induced absolute loss of ~40 Pg soil carbon from the northern permafrost area by 2100. Our findings highlight the need to include fine-scale ecological interactions in order to accurately predict large-scale greenhouse gas emissions, and suggest even tighter restrictions on the estimated 200 Pg anthropogenic carbon emission budget to keep global warming below 1.5°C.

Rapidly rising temperatures spark a biotic awakening of the Arctic that accelerates carbon cycling and may induce a positive feedback to global warming[1–3]. Deepening of the seasonally-thawed surface active layer of permafrost soils is expected to promote the microbial degradation of previously frozen soil organic matter (SOM) to CO_2 or CH_4. At the same time, large areas across the northern permafrost region already show enhanced plant gross primary production (GPP) as a result of rising temperatures and atmospheric CO_2 fertilization[4]. However, existing estimates of broad-scale CO_2 emissions from permafrost soils do not consider interactions between plants and soil microorganisms (**Fig. 1a**).

Plants can accelerate SOM degradation by a mechanism termed the rhizosphere priming effect (RPE; **Fig. 1b**). The RPE is defined as a change in the microbial respiration of soil organic carbon (SOC) affected by plant roots compared to soil without roots, and is the composite effect of enhanced microbial activity by increased carbon availability from root exudates and litter, altered pH values, soil aggregation, and microbial community composition[5–9]. Recent reviews show a stimulation of SOC respiration by up to 380% in experiments with intact plants and by up to 1200% in *in vitro* experiments that simulate the input of plant compounds[5,10]. Both experimental[11] and observational[12–14] evidence suggest persistence of the priming effect over long time frames. Since Arctic soils are vulnerable to the RPE[12,15–20], this raises concern about underestimating future greenhouse gas emissions from permafrost soils in a greening Arctic **(Fig 1c)**.

Quantifying priming-induced carbon losses

Here, we present the first estimate of RPE-induced SOC losses across the northern circumpolar permafrost area under baseline (2010) and future climatic conditions (2100, representative concentration pathways [RCP] 4.5 and 8.5). The aim of this study is two-fold, to provide a robust estimate for the magnitude of RPE including uncertainty analyses, and to

identify key knowledge gaps that should be targeted by future experimental work. The novel *PrimeSCale* model integrates plant root and microbial activities with soil physico-chemical properties at high spatial (5 x 5 km^2) and depth resolution (5 cm intervals down to a max. depth of 3 m). To that end, we combined two meta-analyses of empirical data on the magnitude of the RPE relative to basal and root respiration (**Fig. 1d**) and on root depth distribution in tundra and boreal ecosystems (**Extended Data Fig. 2-4**) with databases and model outputs of SOC storage[21], SOM composition (C/N)[22], GPP[23,24], active layer thickness (ALT)[24], basal SOC respiration rates[24] and vegetation type[25] in the northern circumpolar permafrost area. The combined uncertainties are accounted for using Markov chain Monte Carlo simulations (see **Methods** as well as **Extended Data Fig. 1** and **Supplementary Table 1** for details of model setup and input data).

The impact of plant roots on SOC respiration was quantified based on a meta-analysis of experimental studies that specifically measured RPE induced by intact plants (n = 65; **Supplementary Table 2**). Our meta-analysis showed that SOC respiration from plant-affected soil was on average higher than from unaffected soil by a factor of 1.54 ± 0.54 (mean ± standard deviation; "RPE ratio"). This range is in line with *in vitro* experiments on permafrost soils that substitute intact plants by addition of plant-derived organic compounds[16]. The meta-analysis further revealed a significant, positive relationship between the RPE ratio and root respiration, as a proxy for root activity (**Fig. 1d**). We applied this relationship in the *PrimeSCale* model to derive RPE ratios for individual vegetated grid cells and soil depth increments (**Fig. 2**), with root respiration for each grid cell estimated from GPP and proportionally assigned to individual soil depth increments using rooting-depth distribution functions. In a second meta-analysis (n = 66; **Supplementary Table 3**) we generated separate ALT-dependent rooting-depth distribution functions for erect-shrub, prostrate-shrub, wetland and graminoid tundra and boreal forest, all within the northern

permafrost domain (**Extended Data Fig. 2**). These functions account for denser plant rooting in the shallow soil and an increase in plant rooting depth with active layer deepening (**Extended Data Fig. 2-4**). Under current conditions, 90% of roots are in the top 1.1 m in boreal forest and 0.7 m in tundra. Due to shifts in vegetation and active layer deepening these values are projected to increase by 2100 to 1.2 m and 0.8 m in the RCP 4.5 scenario, and to 1.4 m and 1.1 m in the RCP 8.5 scenario (**Fig. 2b**). Finally, spatial and depth-explicit basal SOC respiration rates (**Supplementary Table 4**) derived from the Community Land Model[24] were combined with RPE ratios for each grid cell and depth increment, to calculate absolute rates of additional SOC respiration induced by the RPE (**Fig. 2c-e**).

Rhizosphere priming amplifies permafrost soil carbon loss

By accounting for interactions between spatial and depth distributions of seasonally unfrozen SOC and roots, and the spatial distribution of GPP, the *PrimeSCale* model permits a first broad-scale assessment of the magnitude of the RPE in natural ecosystems. Across the study area, we estimate that the RPE induces additional SOC respiration of 0.40 Pg yr^{-1} (10 – 90% CI, 0.06 – 0.79Pg yr^{-1}) under 2010 conditions, and of 0.43 Pg yr^{-1} (0.07 – 0.87 Pg yr^{-1}; RCP 4.5) and 0.49 Pg yr^{-1} (0.07 – 0.99 Pg yr^{-1}; RCP 8.5) in 2100 (**Table 1, Fig. 3d-f**). At present, RPE-induced SOC respiration is strongly dominated by the shallow soil with 84% from layers less than 20 cm deep (>95% from layers less than 40 cm deep). Although RPE depth is projected to increase until 2100 due to increasing ALT and consequently deeper rooting, 69% of RPE-induced SOC respiration still derives from soil layers less than 20 cm deep (89% from layers less than 40 cm deep; RCP 8.5) (**Fig. 2**). The absolute increase over time for both RCPs results from a general increase in SOC respiration rates due to climate warming. The relative importance of the RPE remains largely stable over time from an average RPE-ratio of 1.14 in 2010, to 1.13 (RCP 4.5) or 1.11 (RCP 8.5) by 2100 (**Fig. 3a-c**). Overall, we estimate that the

RPE will provoke the cumulative absolute loss of 38 Pg SOC (5.9 –75 Pg; RCP 4.5) or 40 Pg SOC (6.0 – 80 Pg; RCP 8.5) to the atmosphere between 2010 and 2100 (**Fig. 3d-f**; **Table 1**).

Since the occurrence of the RPE might depend on the quality of SOM, and in particular on a limitation of soil microorganisms by low C availability[7,16,26], we performed a sensitivity analysis under the assumption that only SOM with a C/N ratio below 20 is susceptible to the RPE (**Supplementary Table 5**). This sensitivity analysis resulted in lower but still substantial estimates of RPE-induced SOC loss of 27 Pg (4.3 – 55 Pg, RCP 4.5) and 28 Pg (4.2 – 60 Pg, RCP 8.5) between 2010 and 2100 (**Fig. 3g-i**; **Table 1**). Although the theory behind the assumption of a microbial C limitation requirement matches many experimental findings, we emphasize that individual studies observed priming also at high C/N (organic soils)[27–29]. We therefore consider this a sensitivity analysis and highlight the need to target priming at high C/N in experimental studies.

Estimated RPE-induced SOC-respiration showed high spatial variability across the northern circumpolar permafrost region (**Fig. 3, Extended Data Fig. 6**). Regression analysis revealed soil and vegetation characteristics as primary drivers of this variation (R^2 = 0.10-0.70) as opposed to climate and topography, with maxima in areas with high SOC stocks and change in GPP. In the no C/N threshold scenario, RPE-induced SOC-respiration was strongly correlated to occurrence of peat soils (Histels; R^2 = 0.33) owing to the high SOC density in this soil type. Assuming that microbial C limitation is a requirement for priming (threshold scenario) reduced the importance of peat soils (which typically have high C/N) but revealed a strong correlation with the occurrence of cryoturbation that also promotes high SOC storage (Turbels, R^2 = 0.37) (**Supplementary Table 6**). Overall, we identify hot spots of RPE losses in lowlands within the boreal forest biome, including the Hudson Bay, Mackenzie and West Siberian Lowlands, as well as large areas across eastern Siberia (**Fig. 3**).

Reducing uncertainties of priming-induced carbon losses

While the *PrimeSCale* model is based on our current understanding of the RPE and permafrost soils, it also highlights knowledge gaps for which a paucity of empirical data for meta-analysis or inconclusive relations prevent their robust incorporation into broad-scale models: (i) Low temperatures and frequent anoxia in permafrost soils might affect the magnitude of the RPE[30], and geochemical and mineral changes related to permafrost thaw might further affect mineral protection of SOC, and in turn the RPE[5,9,31]. (ii) Our model does not consider leaching of dissolved organic carbon to the deeper soil. Given also the strong priming potential of deep mineral soil horizons observed in *in vitro* experiments[16], leaching of easily available substrate could induce a priming effect that is not restricted to the vicinity of roots[32]. (iii) We assumed that rooting patterns follow an ALT-dependent dose-response curve[33], which strongly constrains the influence of roots on deeper soil layers. Recent field experiments suggest, however, that permafrost thaw might promote deeper rooting of some plant species[34–36] to exploit plant-available nutrients at the permafrost thaw-front[35,37,38]. Further, (iv) while we included spatial variation in GPP and differences in rooting patterns between different tundra vegetation types and boreal forest as well as future changes in vegetation distribution[39], we did not incorporate potential changes in the relative allocation of GPP to roots[35] or different mycorrhizal type associations. While many studies suggest a role of mycorrhiza in priming[13,14,40,41] and spatial products for mycorrhizal type distribution exist[42], mycorrhizal type is not considered in our model since mycorrhizal type effects on soil C-sequestration are highly context dependent[43]. Lastly, (v) potential future change in functional microbial diversity is not addressed, although recent literature shows that microbial communities in newly thawed permafrost soils differ from those in active layer soils[44,45] and upon thaw are vulnerable to change in both community composition[45,46] and likely

functioning[46–48]. Given the large potential impact of RPE on global permafrost SOC losses, these current uncertainties should urgently be targeted by experimental studies.

Implications for the global carbon budget

Our results demonstrate the importance of the rhizosphere priming effect for future carbon releases from permafrost-affected soils to the atmosphere. The estimated RPE-induced ~40 Pg SOC loss from the northern permafrost area until 2100 (RCP 8.5) is additional to permafrost carbon losses due to active layer deepening and increasing soil temperatures, currently estimated at 57 Pg C (range 28-113 Pg; RCP 8.5)[3] over the same period. Moreover, the magnitude of RPE-induced greenhouse gas emissions is in the same range or even exceeds those from other key processes in the northern permafrost region, e.g. from abrupt permafrost collapse[49] or methane release from lakes, ponds[50] and the Arctic Ocean[51] (**Supplementary Table 7**). Remaining knowledge gaps emphasize the need for further studies of plant-microbe interactions in permafrost-affected soils. The RPE-induced permafrost carbon release to the atmosphere is currently unaccounted for in global emission scenarios and implies that the remaining anthropogenic carbon budget to keep warming below 1.5 or 2°C, currently estimated at 200 and 430 Pg C, respectively[52] , may need to be even more constrained.

References

1. McGuire, A. D. *et al.* Dependence of the evolution of carbon dynamics in the northern permafrost region on the trajectory of climate change. *Proc. Natl. Acad. Sci.* **115**, 3882-2887 (2018).
2. Schuur, E. A. G. *et al.* Climate change and the permafrost carbon feedback. *Nature* **520**, 171–179 (2015).
3. Koven, C. D. *et al.* A simplified, data-constrained approach to estimate the permafrost carbon-climate feedback. *Philos. Trans. R. Soc. -Math. Phys. Eng. Sci.* **373**, 20140423 (2015).
4. Xu, L. *et al.* Temperature and vegetation seasonality diminishment over northern lands. *Nat. Clim. Change* **3**, 581–586 (2013).
5. Huo, C., Luo, Y. & Cheng, W. Rhizosphere priming effect: A meta-analysis. *Soil Biol. Biochem.* **111**, 78–84 (2017).
6. Bingeman, C., Varner, J. & Martin, W. The effect of the addition of organic materials on the decomposition of an organic soil. *Soil Sci. Soc. Am. J.* **17**, 34 (1953).
7. Fontaine, S. *et al.* Stability of organic carbon in deep soil layers controlled by fresh carbon supply. *Nature* **450**, 277–280 (2007).
8. Kuzyakov, Y., Friedel, J. K. & Stahr, K. Review of mechanisms and quantification of priming effects. *Soil Biol. Biochem.* **32**, 1485–1498 (2000).
9. Keiluweit, M. *et al.* Mineral protection of soil carbon counteracted by root exudates. *Nat. Clim. Change* **5**, 588–595 (2015).
10. Zhang, W., Wang, X. & Wang, S. Addition of external organic carbon and native soil organic carbon decomposition: a meta-analysis. *PLoS ONE* **8**, e54779 (2013).
11. Dijkstra, F. A. & Cheng, W. Interactions between soil and tree roots accelerate long-term soil carbon decomposition. *Ecol. Lett.* **10**, 1046–1053 (2007).

12. Hartley, I. P. *et al.* A potential loss of carbon associated with greater plant growth in the European Arctic. *Nat. Clim. Change* **2**, 875–879 (2012).
13. Parker, T. C., Subke, J.-A. & Wookey, P. A. Rapid carbon turnover beneath shrub and tree vegetation is associated with low soil carbon stocks at a subarctic treeline. *Glob. Change Biol.* **21**, 2070–2081 (2015).
14. Sulman, B. N. *et al.* Feedbacks between plant N demand and rhizosphere priming depend on type of mycorrhizal association. *Ecol. Lett.* **20**, 1043–1053 (2017).
15. Wild, B. *et al.* Input of easily available organic C and N stimulates microbial decomposition of soil organic matter in arctic permafrost soil. *Soil Biol. Biochem.* **75**, 143–151 (2014).
16. Wild, B. *et al.* Plant-derived compounds stimulate the decomposition of organic matter in arctic permafrost soils. *Sci. Rep.* **6**, 25607 (2016).
17. Pegoraro, E. *et al.* Glucose addition increases the magnitude and decreases the age of soil respired carbon in a long-term permafrost incubation study. *Soil Biol. Biochem.* **129**, 201–211 (2019).
18. Rousk, K., Michelsen, A. & Rousk, J. Microbial control of soil organic matter mineralization responses to labile carbon in subarctic climate change treatments. *Glob. Change Biol.* **22**, 4150–4161 (2016).
19. Walz, J., Knoblauch, C., Boehme, L. & Pfeiffer, E.-M. Regulation of soil organic matter decomposition in permafrost-affected Siberian tundra soils - Impact of oxygen availability, freezing and thawing, temperature, and labile organic matter. *Soil Biol. Biochem.* **110**, 34–43 (2017).
20. Hartley, I. P., Hopkins, D. W., Sommerkorn, M. & Wookey, P. A. The response of organic matter mineralisation to nutrient and substrate additions in sub-arctic soils. *Soil Biol. Biochem.* **42**, 92–100 (2010).

21. Hugelius, G. *et al.* Estimated stocks of circumpolar permafrost carbon with quantified uncertainty ranges and identified data gaps. *Biogeosciences* **11**, 6573–6593 (2014).
22. Harden, J. W. *et al.* Field information links permafrost carbon to physical vulnerabilities of thawing. *Geophys. Res. Lett.* **39**, L15704 (2012).
23. Beer, C. *et al.* Terrestrial gross carbon dioxide uptake: global distribution and covariation with climate. *Science* **329**, 834–839 (2010).
24. Koven, C. D., Lawrence, D. M. & Riley, W. J. Permafrost carbon-climate feedback is sensitive to deep soil carbon decomposability but not deep soil nitrogen dynamics. *Proc. Natl. Acad. Sci. U. S. A.* **112**, 3752–7 (2015).
25. Walker, D. A. *et al.* The Circumpolar Arctic vegetation map. *J. Veg. Sci.* **16**, 267–282 (2005).
26. Bengtson, P., Barker, J. & Grayston, S. J. Evidence of a strong coupling between root exudation, C and N availability, and stimulated SOM decomposition caused by rhizosphere priming effects. *Ecol. Evol.* **2**, 1843–1852 (2012).
27. Walker, T. N. *et al.* Vascular plants promote ancient peatland carbon loss with climate warming. *Glob. Change Biol.* **22**, 1880–1889 (2016).
28. Basiliko, N., Stewart, H., Roulet, N. T. & Moore, T. R. Do root exudates enhance peat decomposition? *Geomicrobiol. J.* **29**, 374–378 (2012).
29. Gavazov, K. *et al.* Vascular plant-mediated controls on atmospheric carbon assimilation and peat carbon decomposition under climate change. *Glob. Change Biol.* **24**, 3911–3921 (2018).
30. Knoblauch, C., Beer, C., Liebner, S. & Grigoriev, M. N. Methane production as key to the greenhouse gas budget of thawing permafrost. *Nat. Clim. Change* **8**, 309–312 (2018).
31. Gentsch, N. *et al.* Temperature response of permafrost soil carbon is attenuated by mineral protection. *Glob. Change Biol.* 3401–3415 (2018).

276 32. Kuzyakov, Y. Priming effects: Interactions between living and dead organic matter. *Soil*
277 *Biol. Biochem.* **42**, 1363–1371 (2010).
278 33. Schenk, H. J. & Jackson, R. B. The global biogeography of roots. *Ecol. Monogr.* **72**, 311–
279 328 (2002).
280 34. Keuper, F. *et al.* Experimentally increased nutrient availability at the permafrost thaw
281 front selectively enhances biomass production of deep-rooting subarctic peatland species.
282 *Glob. Change Biol.* **23**, 4257–4266 (2017).
283 35. Blume-Werry, G., Milbau, A., Teuber, L. M., Johansson, M. & Dorrepaal, E. Dwelling in
284 the deep - strongly increased root growth and rooting depth enhance plant interactions
285 with thawing permafrost soil. *New Phytol.* **223**, 1328–1339 (2019).
286 36. Finger, R. A. *et al.* Effects of permafrost thaw on nitrogen availability and plant-soil
287 interactions in a boreal Alaskan lowland. *J. Ecol.* **104**, 1542–1554 (2016).
288 37. Keuper, F. *et al.* A frozen feast: Thawing permafrost increases plant-available nitrogen in
289 subarctic peatlands. *Glob. Change Biol.* **18**, 1998–2007 (2012).
290 38. Wild, B. *et al.* Amino acid production exceeds plant nitrogen demand in Siberian tundra.
291 *Environ. Res. Lett.* **13**, 034002 (2018).
292 39. Pearson, R. G. *et al.* Shifts in Arctic vegetation and associated feedbacks under climate
293 change. *Nat. Clim. Change* **3**, 673–677 (2013).
294 40. Lindahl, B. D. & Tunlid, A. Ectomycorrhizal fungi - potential organic matter
295 decomposers, yet not saprotrophs. *New Phytol.* **205**, 1443–1447 (2015).
296 41. Zak, D. R. *et al.* Exploring the role of ectomycorrhizal fungi in soil carbon dynamics.
297 *New Phytol.* **223**, 33–39 (2019).
298 42. Soudzilovskaia, N. A. *et al.* Global mycorrhizal plant distribution linked to terrestrial
299 carbon stocks. *Nat. Commun.* **10**, 1–10 (2019).
300 43. Tedersoo, L. & Bahram, M. Mycorrhizal types differ in ecophysiology and alter plant
301 nutrition and soil processes. *Biol. Rev.* **94**, 1857–1880 (2019).

44. Hultman, J. *et al.* Multi-omics of permafrost, active layer and thermokarst bog soil microbiomes. *Nature* **521**, 208-212 (2015).
45. Monteux, S. *et al.* Long-term in situ permafrost thaw effects on bacterial communities and potential aerobic respiration. *ISME J* **12**, 2129–2141. (2018).
46. Mackelprang, R. *et al.* Metagenomic analysis of a permafrost microbial community reveals a rapid response to thaw. *Nature* **480**, 368-U120 (2011).
47. Johnston, E. R. *et al.* Responses of tundra soil microbial communities to half a decade of experimental warming at two critical depths. *Proc. Natl. Acad. Sci. U. S. A.* **116**, 15096–15105 (2019).
48. Monteux, S. A song of ice and mud: Interactions of microbes with roots, fauna and carbon in warming permafrost-affected soils. (2018).
49. Turetsky, M. R. *et al.* Carbon release through abrupt permafrost thaw. *Nat. Geosci.* **13**, 138–143 (2020).
50. Wik, M., Varner, R. K., Anthony, K. W., MacIntyre, S. & Bastviken, D. Climate-sensitive northern lakes and ponds are critical components of methane release. *Nat. Geosci.* **9**, 99–105 (2016).
51. Shakhova, N. *et al.* Ebullition and storm-induced methane release from the East Siberian Arctic Shelf. *Nat. Geosci.* **7**, 64–70 (2014).
52. Goodwin, P. *et al.* Pathways to 1.5°C and 2°C warming based on observational and geological constraints. *Nat. Geosci.* **11**, 102–107 (2018).

Corresponding authors

Correspondence should be addressed to Frida Keuper (frida.keuper@inrae.fr) and Birgit Wild (birgit.wild@aces.su.se).

Acknowledgements

We thank P. Thornton, F. Dijkstra, Y. Carrillo and R. E. Hewitt for providing additional information on published data. Fig. 1a-c is courtesy of R. Miedema (IN Produktie, Amsterdam). This study was supported by funding from the Swedish Research Council (VR; Grant no. 621-2011-5444), Formas (Grant no. 214-2011-788), and the Knut och Alice Wallenberg Foundation (Grant no. KAW 2012.0152) awarded to E.D.; Academy of Finland funded projects SCART (grant no. 267463) and WASCO (grant no. 305471), Emil Aaltonen Foundation funded project 'eat-less-water', European Research Council (ERC) under the European Union's Horizon 2020 research and innovation programme (grant agreement No. 819202), and *Maa- ja vesitekniikan tuki ry* awarded to M.K.; the JPI Climate Project COUP-Austria (BMWFW-6.020/0008) awarded to A.R.; two projects funded by the Swedish Research Council, the EU JPI-climate COUP project (E0689701) and Project INCA (E0641701) with Marie Sklodowska Curie Actions, Cofund (600398) awarded to G.H.; by the Deutsche Forschungsgemeinschaft (BE 6485/1-1) to C.B.; and by the US DOE BER RGMA program through the RUBISCO SFA and ECRP projects to C. K..

Author contributions

F.K. and E.D. conceived the idea. F.K., B.W. and E.D. led the conceptual model development in collaboration with M.K., C.B., G.B.-W., S.F., K.G., G.G., G.H., E.K., P.K., S.M., A.R and J.W. The model was implemented by M.K. and M.J., and C.B., N.G., G.H., C.K., and P.K. provided additional data. M.K., G.H., C.K., J.W. and E.D. performed additional statistical analyses. F.K. and B.W. wrote the manuscript with contribution of all authors.

Competing interests

The authors declare no competing interests.

Figure captions

Fig. 1. The rhizosphere priming effect (RPE). (**a**) Permafrost soil organic carbon (SOC) respiration without RPE; (**b**) SOC respiration including the RPE under present conditions; (**c**) Future scenario considering climate warming: faster growing plants; deeper active layer; deeper rooting depth. (**d**) The RPE ratio (SOC respiration from plant-affected over not plant-affected soils) vs root respiration, an indicator for plant root activity. Data are from meta-analysis of studies quantifying RPE in experiments with intact plants, representing 65 individual treatment combinations. The dotted line indicates an RPE ratio of 1, i.e. no RPE, with observed positive RPE above and negative RPE below.

Fig. 2. Depth distribution of soil and root properties, and the RPE. Averages across (**b-d**) or summed over (**a, e**) the northern circumpolar permafrost region, of (**a**) total SOC stock and SOC stocks above the ALT in 2010 and 2100 (RCP 8.5); (**b**) plant root percentage and cumulative percentage in 2010 and 2100; (**c**) soil respiration without the RPE; (**d**) RPE ratios (SOC respiration from plant-affected over not plant-affected soils) in seasonally unfrozen and vegetated soils and (**e**) absolute annual RPE-induced SOC losses in 2010 and 2100. Uncertainty ranges are included for c-e. See **Extended Data Fig. 1** for model structure.

Fig. 3. Spatial distribution of the RPE across the northern circumpolar permafrost region in 2010 and 2100 (RCP 4.5 and 8.5). (**a-c**) Distribution of the RPE ratio and (**d-i**) of the absolute annual RPE-induced SOC loss (in Mg C km^{-2} yr^{-1}), assuming that (**d-f**) all plant-affected SOC is susceptible to the RPE (no C/N threshold scenario) or that (**g-i**) microbial carbon limitation is required (C/N threshold scenario). See **Extended Data Fig. 6** for coefficients of variation.

373 **Tables**

Table 1. Annual and cumulative RPE-induced SOC respiration from the northern circumpolar permafrost area in 2010 and 2100 (RCP 4.5 and 8.5). The RPE-induced SOC respiration was calculated in two scenarios, assuming that all plant-affected SOC is susceptible to the RPE (no C/N threshold scenario) or that microbial carbon limitation is required (C/N threshold scenario). Values are means for Monte Carlo (N = 1000) simulations (10% – 90% confidence intervals).

	2010	2100 [RCP 4.5]	2100 [RCP 8.5]
Annual RPE-induced SOC respiration (Pg yr^{-1})			
No C/N threshold scenario	0.40 (0.06 – 0.79)	0.43 (0.07 – 0.87)	0.49 (0.07 – 0.99)
C/N Threshold scenario	0.28 (0.05 – 0.60)	0.31 (0.05 – 0.61)	0.34 (0.05 – 0.74)
Cumulative RPE-induced SOC respiration (Pg)			
No C/N threshold scenario		38 (5.9 – 75)	40 (6.0 – 80)
C/N Threshold scenario		27 (4.3 – 55)	28 (4.2 – 60)

374

Methods

Overview of the PrimeSCale model

The *PrimeSCale* model was developed to quantify soil organic carbon (SOC) respiration induced by the rhizosphere priming effect (RPE) on large spatial scales and with high depth resolution, while accounting for interactions between spatial and depth distributions of plant-carbon inputs and SOC content and quality. The model represents current peer-reviewed RPE knowledge only, i.e. potential mechanisms for which evidence is inconclusive or where data are too scarce for meaningful meta-analysis are not included. The model thus reveals knowledge gaps, which are discussed in the manuscript section 'Reducing uncertainties of priming-induced carbon losses'. The relatively simple model structure allows for rapid integration of new data when available (**Extended Data Fig. 1**).

The current study focuses on the terrestrial northern circumpolar permafrost area, defined by the overlapping extent of permafrost terrain in the Circum-Arctic Map of Permafrost and Ground-Ice Conditions[53] and the Northern Circumpolar Soil Carbon Database[54,55]. After masking out all non-vegetated areas, i.e. barren land, rocklands, land ice (glaciers and ice-sheets), and freshwater, the study area covers 14 million km^2, around 12% of the global ice-free land area. The model's spatial resolution is 5 km x 5 km, and the study area includes 561,956 active grid cells. We considered only the top 3 m of the soil, where the vast majority of plant roots is located[33]. The 0-3 m soil column was divided into 5 cm thick layers, resulting in 60 soil layers. We thus modelled the RPE in 33.7 million grid cubes with a dimension of 5 km x 5 km x 5 cm. Results were reported either as global values, as averages over soil layers for each grid cell to derive maps, or as averages over grid cells for each soil layer to derive depth profile figures.

We estimated current (year 2010), future (year 2100) and cumulative (2010 – 2100) RPE-induced SOC losses under the representative concentration pathway (RCP) scenarios 4.5 and

8.5, considering projected changes in active layer thickness (ALT), gross primary production (GPP), vegetation distribution and growing season length based on existing models. To estimate the cumulative RPE-induced SOC losses, we assumed linear changes in ALT, vegetation distribution and GPP per growing season day for each grid cell until 2100. An overview of all input data and model parameters is given in **Supplementary Table 1**. The PrimeSCale model is structured in three modules: Soil, Plant and Soil Respiration. The model setup is outlined in **Extended Data Fig. 1**.

Soil Module

Soil organic C stocks of the northern permafrost area

Data on SOC stocks were derived from the Northern Circumpolar Soil Carbon Database[21,54,55], at a spatial resolution of 5 km x 5 km and a depth resolution of 5 cm, to a maximum depth of 3 m. We used data from all three Gelisol suborders (Histels, Orthels, Turbels), and distinguished three soil horizon types: organic, cryoturbated and mineral[22]. Note that the discontinuity in SOC stocks at 1 m (**Fig. 2a)** is due to a potential sampling bias in the Northern Circumpolar Soil Carbon Database[21,55]. For each of the soil horizon types, SOC was summed over the three Gelisol suborders. Soil organic carbon stocks are stable over time in our model, creating a ~3% overestimation of the entire carbon pool by 2100 as estimated from CLM projections of SOC changes[56]. The SOC stocks for the three soil horizon types are presented in **Extended Data Fig. 7**.

Active layer depth

The thickness of the seasonally thawed active layer at the surface of permafrost soils (ALT; active layer thickness) was calculated based on CLM4.5 simulations[24]. The suitability of

CLM for this purpose has been previously described and confirmed[57]. We used 11-year average ALT values for the years 2010 (2006-2016) and 2100 (2095-2105) under the RCP4.5 and RCP8.5 scenarios (**Extended Data Fig. 7**).

Soil organic matter C/N ratios

Previous studies in permafrost and other soils suggest that C limitation of soil microorganisms might be a requirement for the RPE[15,16,26,58]. We therefore calculated RPE-induced SOC respiration for two scenarios: (i) in the "no threshold scenario", we assumed that RPE is independent of microbial C limitation; (ii) in the "threshold scenario", we assumed that microbial C limitation is required for the RPE. Microbial C limitation has been suggested to occur where the C/N ratio of SOM is below a Threshold Elemental Ratio, that is estimated to fall between 20 and 27 (mol/mol)[59–61]. For the threshold scenario, we thus used a threshold C/N ratio of 20 which is at the lower end of the suggested range, i.e. more conservative, and assumed that SOM with a C/N ratio above this threshold is not susceptible to the RPE (RPE ratio = 1). The threshold scenario serves as a sensitivity analysis; presented data refer to the no threshold scenario unless specified otherwise. We estimated the fraction of soil horizons that fall above or below this threshold based on observational data (N = 472) compiled from previous studies[22,62] and extensive unpublished data from G. Hugelius and P. Kuhry. The observational data were grouped by soil horizon type and depth in the soil column to extract the fraction of observations that fell above the C/N threshold of 20 (**Supplementary Table 5**).

Plant Module

RPE ratio function

448 The RPE is driven by the transfer of fresh organic compounds from plants to the soil, and is
449 consequently expected to show a positive relationship to plant root activity. To describe this
450 relationship, we conducted a meta-analysis of published studies (retrieved from the Web of
451 Science, 10.10.2016) that report on experiments with intact, potted plants that were
452 continuously labelled with ^{13}C-depleted CO_2. In such an experimental setup, the ^{13}C-depleted
453 part of respired CO_2 is derived from the plants themselves or plant-associated microorganisms
454 that thrive on plant root exudates or litter (further termed plant-associated respiration),
455 whereas non-depleted CO_2 comes from SOC decomposition (further termed SOC respiration).
456 Our meta-analysis included only studies where (a) plants were grown in natural soils, (b)
457 plants were continuously labelled with ^{13}C-depleted CO_2, and in which (c) SOC respiration
458 from planted pots, (d) SOC respiration from unplanted control pots, and (e) either total or
459 belowground plant-associated respiration were published or could be obtained from the
460 authors.

461 We refrained from including studies that were not based on experiments with isotopically
462 labelled living plants, but instead simulate plant-soil C transfer by adding one or few
463 isotopically labelled organic substrates to the soil. While such a reduced experimental setup is
464 a prerequisite for dissecting the mechanisms underlying RPE[10], only experiments using living
465 plants capture the full natural range of soil modifications by plants (continuous exudation of a
466 wide range of chemical compounds released by plants, changes in nutrient and water
467 availability, pH, soil aggregation, and microbial community composition)[63,64], and allow us to
468 link the magnitude of RPE to estimates of root activity.

469 The dataset used for meta-analysis consisted of 12 studies on intact plants and comprised 65
470 individual treatment combinations (i.e., combinations of soil, plant species, and growth
471 conditions, **Supplementary Table 2**). All studies reported total or belowground plant
472 associated respiration, which we converted into root respiration (See **Supplementary**

473 **Methods**). All soils were mineral soils, most soils and plant species were derived from
474 temperate ecosystems, and temperatures during experiments were in the range of 15-20°C
475 (night) and 25-28°C (day). No studies were available that included arctic or subarctic soils or
476 plants. To minimize potential biases introduced by differences between temperate and arctic
477 systems, we normalized RPE by calculating RPE ratios, as (unlabelled) SOC respiration in
478 planted pots divided by SOC respiration in unplanted control pots. We thus aimed to reduce
479 effects of parameters such as temperature, organic matter quantity or quality that drive
480 differences in absolute SOC respiration between systems.

481 The RPE ratios in our meta-analysis ranged from 0.39 to 3.15 (note that RPE-ratio values
482 below 1 represent negative priming), with a mean value of 1.54 (± 0.54 standard deviation).
483 These values fall well in line with other recent global meta-analyses of RPE in intact plant
484 experiments (mean 1.59)[5] and substrate addition experiments (mean 1.27)[10], and, importantly,
485 with RPE ratios measured in 119 arctic permafrost soils after substrate addition (cellulose
486 addition: mean 1.21; protein addition: mean 1.81)[16].

487 Our meta-analysis showed a positive relationship between RPE ratio and root respiration (mg
488 C kg^{-1} soil d^{-1}) across all studies which we described with a saturating (Michaelis-Menten)
489 function fit with Markov chain Monte Carlo methods assuming gamma priors on both fitted
490 parameters, and Normal distributed errors (**Extended Data Fig. 8**). Since we assumed neither
491 positive nor negative priming at root respiration = 0 we fixed the intercept at 1. The
492 Michaelis-Menten fit showed a lower root mean square error than a linear model implying
493 better in-sample prediction performance, and is additionally supported by previous substrate
494 addition experiments where a similar relationship was observed between the amount of
495 substrate added and their utilization by the microbial community[65,66]. The posterior medians
496 of the two fitted parameters yielded the following empirical relationship between RPE and
497 root respiration:

$$RPE\text{-}ratio = 1 + \frac{2.47 * root\ respiration}{13.01 + root\ respiration} \quad (1)$$

This RPE ratio function was applied in the *PrimeSCale* model to calculate RPE ratios for each grid cube, using root respiration estimates derived from GPP that were spread over the soil column employing the root depth distribution functions.

Gross primary production

Current annual GPP across the northern permafrost area was derived from ref.[23] at a resolution of 0.5°. Future GPP in the year 2100 was estimated for RCP 4.5 and RCP 8.5 scenarios, by applying the relative change in GPP CLM4.5[24] as a result of rising temperatures and atmospheric CO_2 fertilization to the current GPP estimate, thus preserving the higher spatial resolution of ref.[23]. Annual GPP values[23,24] were converted into daily GPP values for the growing season by dividing annual GPP values by growing season length[67]. For details on calculation of future GPP and conversion to daily values see **Supplementary Methods**. The final GPP maps are presented in **Extended Data Fig. 7**.

Root respiration

Root respiration was used as a proxy for plant belowground C allocation in order to estimate RPE and calculated both (1) for grid cells of the model area, based on GPP data (**Extended Data Fig. 5**), and (2) as a common output unit for studies used in the RPE ratio meta-analysis, based on total plant-associated respiration (respiration by whole plants and root associated microorganisms) or belowground plant-associated respiration (respiration by roots and root associated microorganisms) depending on which was reported in the respective study (**Extended Data Fig. 8; Supplementary Table 2**). We derived conversion factors from previously published extensive meta-analyses on different aspects of plant C allocation,

including GPP[68], total and belowground plant-associated respiration[69], as well as root respiration[70]. Overall, we estimated root respiration as 3.6% of GPP, 7.4% of total plant-associated respiration, and 48% of belowground plant-associated respiration. Starting from current and future GPP data, we thus approximated root activity in each grid cell of the study area, which we spread over depth using soil bulk density data (See **Supplementary Methods**; **Supplementary Table 8**) and root distribution functions (below). Via the RPE ratio function we calculated, for each grid cube, the expected RPE ratio at its root activity. For further details on calculation of root respiration and application in the PrimeSCale model see **Supplementary Methods**.

Root depth distribution functions

Root density, and consequently the potential for RPE, decrease with soil depth in natural ecosystems. Root depth distribution functions were therefore applied in the *PrimeSCale* model to proportionally spread root respiration estimates (see **Supplementary Methods**) over the soil depth profile. We derived root depth distribution functions for five vegetation types within the northern permafrost area by a meta-analysis of studies on root depth distribution in natural arctic and subarctic tundra systems, as well as in boreal forests, all on permafrost soils. We included only studies where root data from at least three soil depths were reported, where information on active layer thickness could be retrieved, and where roots from either the entire vegetation or from all individual species at the site were analysed; in the latter case, individual species data were summed to retrieve combined root profiles for the respective site.

Following Schenk and Jackson[33] we fitted logistic dose-response functions for each profile:

$$r(D) = \frac{100}{1+\left(\frac{D}{D50}\right)^{c}} \quad (2)$$

where r(D) is the observed cumulative percentage of roots above depth D, and D50 (representing the depth above which we find 50% of the roots), and c (a dimensionless shape-parameter) are estimated from the data. Given that rooting depth is limited by ALT in permafrost soils[33], we expressed D (and D50) as a fraction of ALT; this allows adjustment of maximum rooting depth according to variations in ALT (spatial variation between the grid cells or changes in ALT between 2010 and 2100).

For a small number of root profile datasets the non-linear regression routine did not converge, usually because of insufficient data points. These profiles were excluded from subsequent analyses resulting in a total of 66 root profiles from 25 individual studies (**Supplementary Table 3**). This meta-analysis represents to our knowledge the first on boreal forests specifically on permafrost, as well as an almost tripling of tundra root profile observations from 20 to 54 profiles compared to a previous study[33]. Subsequently, tundra root profiles were assigned to tundra types (graminoid tundra, erect-shrub tundra, prostrate-shrub tundra and tundra wetland) based on the site description in the original publications and the criteria defined in the Circumpolar Arctic Vegetation Map[25]. Means as well as uncertainty ranges of D50 and c were calculated for each vegetation type: boreal forest (mean D50 = 0.19, mean c = -2.32, n = 12 profiles), graminoid tundra (D50 = 0.28, c = -2.51, n = 20), erect-shrub tundra (D50 = 0.26, c = -2.92, n = 8), prostrate-shrub tundra (D50 = 0.29, c = -2.75, n = 8) and tundra wetlands (D50 = 0.25, c = -3.20, n = 18).

Equation (2) was then used to spread root respiration (equation S1, **Supplementary Methods**) proportionally across the soil depth profile in each vegetation class (**Extended Data Fig. 2-5**), using the corresponding ALT for each grid cell. Vegetation distribution for the tundra biome was based on the present Circumpolar Arctic Vegetation Map[25] and its future projections[39], and the remaining northern permafrost area was classified as boreal forest (**Extended Data Fig. 9**).

570

571 Soil Respiration Module

572 *Basal SOC respiration*

573 Basal SOC respiration without the RPE was calculated for the northern permafrost area using
574 output from the CLM4.5[24], which does not include any explicit RPE terms or dependency of
575 SOM decomposition rates on plant productivity or other biotic factors. In addition, the CLM
576 has been shown to systematically underestimate soil turnover rates in cold biomes[24],
577 potentially, among other factors, due to lack of RPE. The CLM has, however, a relatively
578 coarse spatial resolution and the absolute values of GPP and SOC at any given site are less
579 realistic than those available in the data-based products used in the *PrimeSCale* model (e.g.
580 the CLM model has no peatlands). We therefore calculated basal SOC respiration as a
581 function of GPP, using GPP as a proxy for climatic conditions that favour both GPP and basal
582 SOC respiration[71–73]. We extracted a relationship between GPP and the fraction of total active
583 layer SOC that is heterotrophically respired (Rh/SOC) from permafrost-affected grid cells in
584 the CLM model, and applied this to the high resolution SOC and GPP data used in the
585 *PrimeSCale* model to generate basal SOC respiration values for each individual gridcell. To
586 avoid an overestimation of basal SOC respiration by CO_2-fertilization of GPP in the future
587 (which is independent from the climatic conditions driving respiration), we used GPP data
588 from a CLM simulation without CO_2-fertilization[24] for this purpose. We used quantile
589 regression to fit a model for the median and 10th and 90th percentiles (for uncertainty analysis,
590 see below) of simulated Rh/SOC as a function of simulated GPP, assuming an exponential
591 relationship:

592 $$\frac{Rh}{SOC} = A * GPP^{B} \quad (3)$$

where A and B are model parameters to be estimated. Because of the wide range of individual grid cell-level SOC values predicted by the CLM4.5, we performed an outlier selection to first remove all zero-productivity grid cells and then use only the 10^{th}-90^{th} percentiles of the grid cells as ranked by their initial SOC stocks. Soil respiration (Rh-fraction * SOC) per grid cell was spread over depth using an ALT-dependent depth function extracted from the CLM model (**Extended Data Fig. 10**).

Plant-affected SOC respiration

Plant-affected SOC respiration (i.e., SOC respiration considering the RPE) was calculated by combining RPE ratios (Plant Module) with basal SOC respiration rates (Soil Respiration Module). For grid cubes that were identified as primeable (i.e. seasonally thawed; GPP > 0; and in the case of the microbial C limitation scenario below a C/N threshold of 20), we calculated plant-affected SOC respiration by multiplying their basal SOC respiration estimate with the RPE ratio. For grid cells identified as not primeable, we set the RPE ratio to 1 (i.e., no RPE) so plant-affected SOC respiration equalled basal SOC respiration (i.e. no increase in SOC respiration).

Uncertainty estimates

We used Monte Carlo simulations (n = 1000) to analyse model uncertainties (**Extended Data Fig. 6**), considering the parameters listed in **Supplementary Table 9** and assuming normal distribution for all parameters except SOC and soil bulk density, for which a truncated normal distribution with range [0 - 2*mean] was used to avoid negative values. Confidence intervals (CI) in the main text refer to Monte Carlo Confidence Intervals[74].

Analysis of spatial patterns

We used linear regression to analyse the relationship of the spatial variation in RPE-induced SOC respiration (2100, RCP 8.5) and RPE ratio of both C/N threshold and no threshold scenarios to the spatial variation of 15 potential drivers: characteristics of the vegetation (GPP in 2100; relative change in GPP until 2100), soil (SOC stock in active layer; SOC stock in upper 3 m; distribution of three Gelisol suborders: Histels, Turbels, Orthels), climate (ALT in 2100; change in ALT until 2100; 1970-2000 mean annual average temperature, mean annual precipitation, as well as annual temperature range as a measure of continentality[75]), and terrain (distance to large rivers, distance to lakes, topography[76–78]) (**Supplementary Table 6**).

Data availability

All datasets generated and/or analysed for this study are freely available. References to published data can be found in **Supplementary Table 1** (PrimeSCale model), **Supplementary Table 2** (meta-analysis of priming studies) and **Supplementary Table 3** (meta-analysis of root depth profiles for tundra and boreal), as well as in the main text. Other supporting files are available in the Bolin Centre Database (https://bolin.su.se/data/keuper-wild-2020) and include: a) Input data for the PrimeSCale model (.mat); b) Intermediate output data of the PrimeSCale model (.xls); c) Output (Geotiff) and metadata.

Code availability

The custom code for the PrimeSCale 1.0 model, including model script and complementary function script, is available from the authors upon request, as well as from the Bolin Centre code repository: https://git.bolin.su.se/bolin/keuper-wild-2020.

640 **References**

641 53. Brown, J., Ferrians, O. J. Jr., Heginbottom, J. A. & Melnikov, E. S. Circum-arctic map of
642 permafrost and ground ice conditions, version 2. (2002).
643 54. Hugelius, G. *et al.* The northern circumpolar soil carbon database: Spatially distributed
644 datasets of soil coverage and soil carbon storage in the northern permafrost regions. *Earth*
645 *Syst. Sci. Data* **5**, 3–13 (2013).
646 55. Hugelius, G. *et al.* A new data set for estimating organic carbon storage to 3m depth in
647 soils of the northern circumpolar permafrost region. *Earth Syst. Sci. Data* **5**, 393–402
648 (2013).
649 56. McGuire, A. D. *et al.* Dependence of the evolution of carbon dynamics in the northern
650 permafrost region on the trajectory of climate change. *Proc. Natl. Acad. Sci. U. S. A.* **115**,
651 3882–3887 (2018).
652 57. Lawrence, D. M., Slater, A. G. & Swenson, S. C. Simulation of present-day and future
653 permafrost and seasonally frozen ground conditions in CCSM4. *J. Clim.* **25**, 2207–2225
654 (2012).
655 58. Fontaine, S., Bardoux, G., Abbadie, L. & Mariotti, A. Carbon input to soil may decrease
656 soil carbon content. *Ecol. Lett.* **7**, 314–320 (2004).
657 59. Mooshammer, M. *et al.* Adjustment of microbial nitrogen use efficiency to
658 carbon:nitrogen imbalances regulates soil nitrogen cycling. *Nat. Commun.* **5**, 3694 (2014).
659 60. Sinsabaugh, R. L., Manzoni, S., Moorhead, D. L. & Richter, A. Carbon use efficiency of
660 microbial communities: Stoichiometry, methodology and modelling. *Ecol. Lett.* **16**, 930–
661 939 (2013).
662 61. Sinsabaugh, R. L. *et al.* Stoichiometry of microbial carbon use efficiency in soils. *Ecol.*
663 *Monogr.* **86**, 172–189 (2016).
664 62. Gentsch, N. *et al.* Storage and transformation of organic matter fractions in cryoturbated
665 permafrost soils across the Siberian Arctic. *Biogeosciences* **12**, 4525–4542 (2015).

63. Kuzyakov, Y. Review: Factors affecting rhizosphere priming effects. *J. Plant Nutr. Soil Sci.* **165**, 382–396 (2002).
64. Hinsinger, P., Bengough, A. G., Vetterlein, D. & Young, I. M. Rhizosphere: Biophysics, biogeochemistry and ecological relevance. *Plant Soil* **321**, 117–152 (2009).
65. Jones, D. L. & Murphy, D. V. Microbial response time to sugar and amino acid additions to soil. *Soil Biol. Biochem.* **39**, 2178–2182 (2007).
66. Boddy, E., Roberts, P., Hill, P. W., Farrar, J. & Jones, D. L. Turnover of low molecular weight dissolved organic C (DOC) and microbial C exhibit different temperature sensitivities in Arctic tundra soils. *Soil Biol. Biochem.* **40**, 1557–1566 (2008).
67. FAO/IIASA. Global Agro-ecological zones (GAEZ v3.0). (2010).
68. Zhang, Y., Xu, M., Chen, H. & Adams, J. Global pattern of NPP to GPP ratio derived from MODIS data: Effects of ecosystem type, geographical location and climate. *Glob. Ecol. Biogeogr.* **18**, 280–290 (2009).
69. Jones, D. L., Nguyen, C. & Finlay, R. D. Carbon flow in the rhizosphere: Carbon trading at the soil-root interface. *Plant Soil* **321**, 5–33 (2009).
70. Kuzyakov, Y. & Larionova, A. A. Root and rhizomicrobial respiration: A review of approaches to estimate respiration by autotrophic and heterotrophic organisms in soil. *J. Plant Nutr. Soil Sci.* **168**, 503–520 (2005).
71. Bond-Lamberty, B., Bailey, V. L., Chen, M., Gough, C. M. & Vargas, R. Globally rising soil heterotrophic respiration over recent decades. *Nature* **560**, 80–83 (2018).
72. Bond-Lamberty, B., Wang, C. & Gower, S. T. A global relationship between the heterotrophic and autotrophic components of soil respiration? *Glob. Change Biol.* **10**, 1756–1766 (2004).
73. Hibbard, K. A., Law, B. E., Reichstein, M. & Sulzman, J. An analysis of soil respiration across northern hemisphere temperate ecosystems. *Biogeochemistry* **73**, 29–70 (2005).
74. Buckland, S. T. Monte Carlo confidence intervals. *Biometrics* **40**, 811–817 (1984).

75. Hijmans, R. J., Cameron, S. E., Parra, J. L., Jones, P. G. & Jarvis, A. Very high resolution interpolated climate surfaces for global land areas. *Int. J. Climatol.* **25**, 1965–1978 (2005).
76. Kummu, M., de Moel, H., Ward, P. J. & Varis, O. Data from: How close do we live to water? a global analysis of population distance to freshwater bodies. (2011) doi:10.5061/dryad.71c6r.
77. Kummu, M., Moel, H. de, Ward, P. J. & Varis, O. How close do we live to water? A global analysis of population distance to freshwater bodies. *PLOS ONE* **6**, e20578 (2011).
78. Iwahashi, J. & Pike, R. J. Automated classifications of topography from DEMs by an unsupervised nested-means algorithm and a three-part geometric signature. *Geomorphology* **86**, 409–440 (2007).

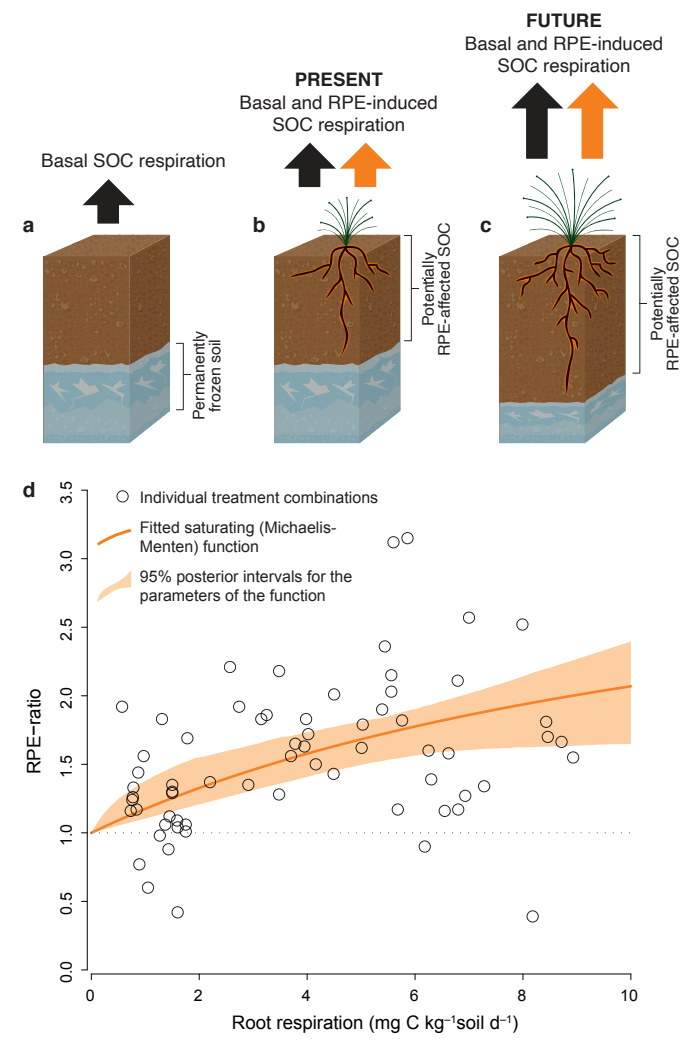
FUTURE
Basal and RPE-induced SOC respiration
PRESENT
Basal and RPE-induced SOC respiration
Basal SOC respiration
a
b
c
Permanently frozen soil
Potentially RPE-affected SOC
Potentially RPE-affected SOC
d
Individual treatment combinations
Fitted saturating (Michaelis-Menten) function
95% posterior intervals for the parameters of the function
RPE−ratio
0.0
0.5
1.0
1.5
2.0
2.5
3.0
3.5
0
2
4
6
8
10
Root respiration (mg C kg⁻¹soil d⁻¹)

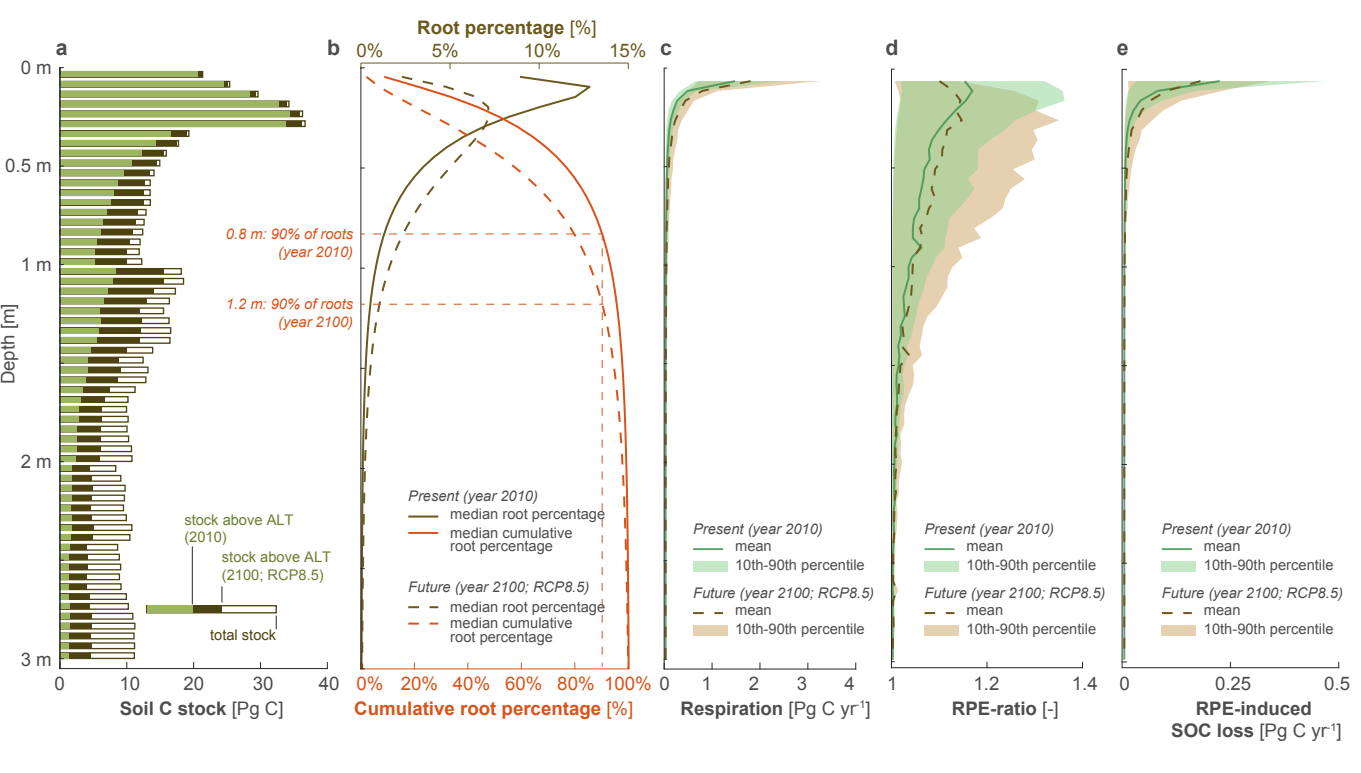
a
b
c
d
e
Root percentage [%]
0%
5%
10%
15%
0 m
0.5 m
1 m
2 m
3 m
Depth [m]
0.8 m: 90% of roots (year 2010)
1.2 m: 90% of roots (year 2100)
stock above ALT (2010)
stock above ALT (2100; RCP8.5)
total stock
Present (year 2010)
median root percentage
median cumulative root percentage
Future (year 2100; RCP8.5)
median root percentage
median cumulative root percentage
Present (year 2010)
mean
10th-90th percentile
Future (year 2100; RCP8.5)
mean
10th-90th percentile
Present (year 2010)
mean
10th-90th percentile
Future (year 2100; RCP8.5)
mean
10th-90th percentile
Present (year 2010)
mean
10th-90th percentile
Future (year 2100; RCP8.5)
mean
10th-90th percentile
0
10
20
30
40
Soil C stock [Pg C]
0%
20%
40%
60%
80%
100%
Cumulative root percentage [%]
0
1
2
3
4
Respiration [Pg C yr-1]
1
1.2
1.4
RPE-ratio [-]
0
0.25
0.5
RPE-induced SOC loss [Pg C yr-1]

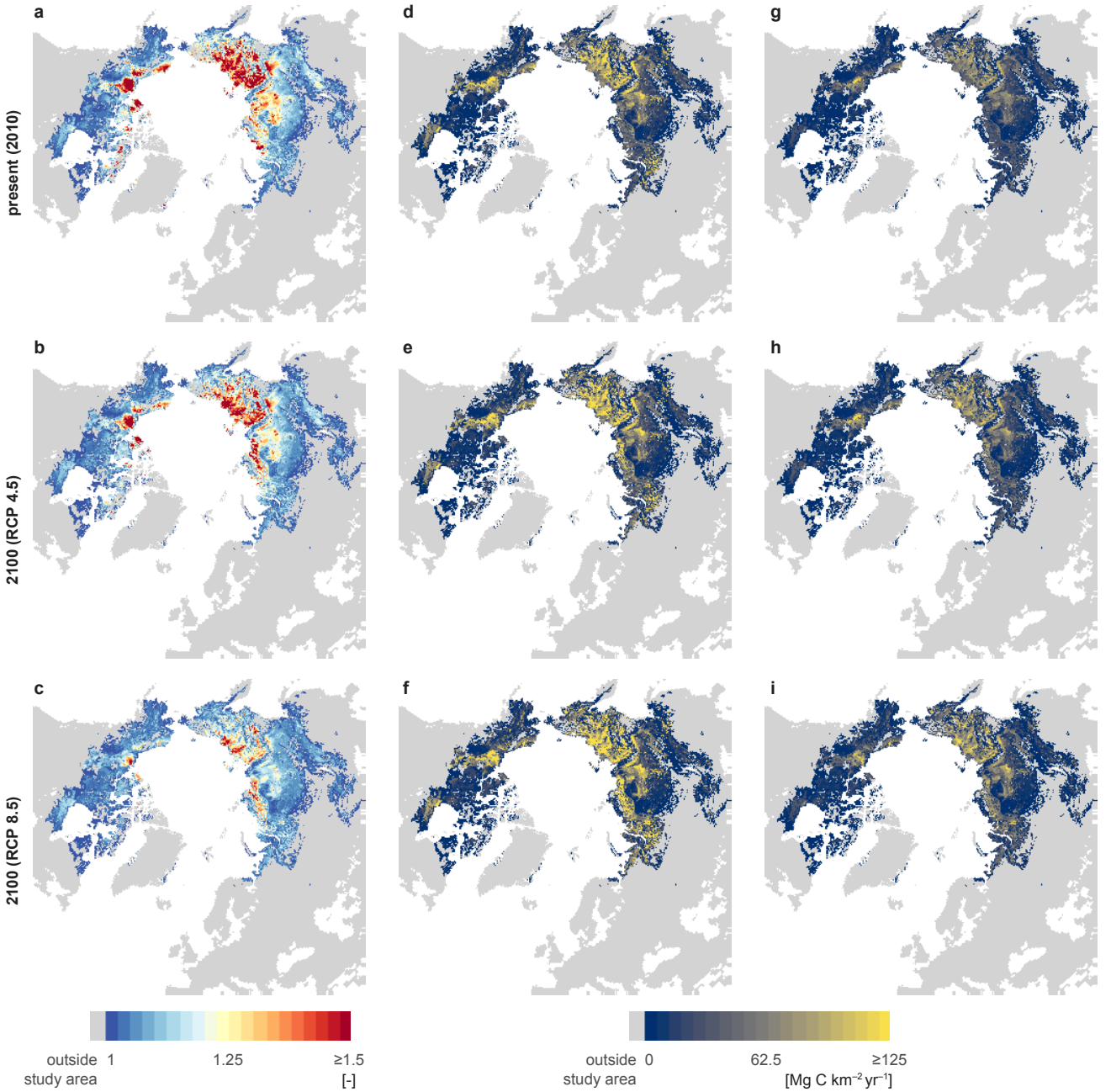
RPE ratio
Mean (n = 1000)
RPE-induced SOC loss
no C/N threshold
Mean (n = 1000)
RPE-induced SOC loss
C/N threshold
Mean (n = 1000)
a
b
c
d
e
f
g
h
i
present (2010)
2100 (RCP 4.5)
2100 (RCP 8.5)
outside study area
1
1.25
≥1.5
[-]
outside study area
0
62.5
≥125
[Mg C km−2 yr−1]

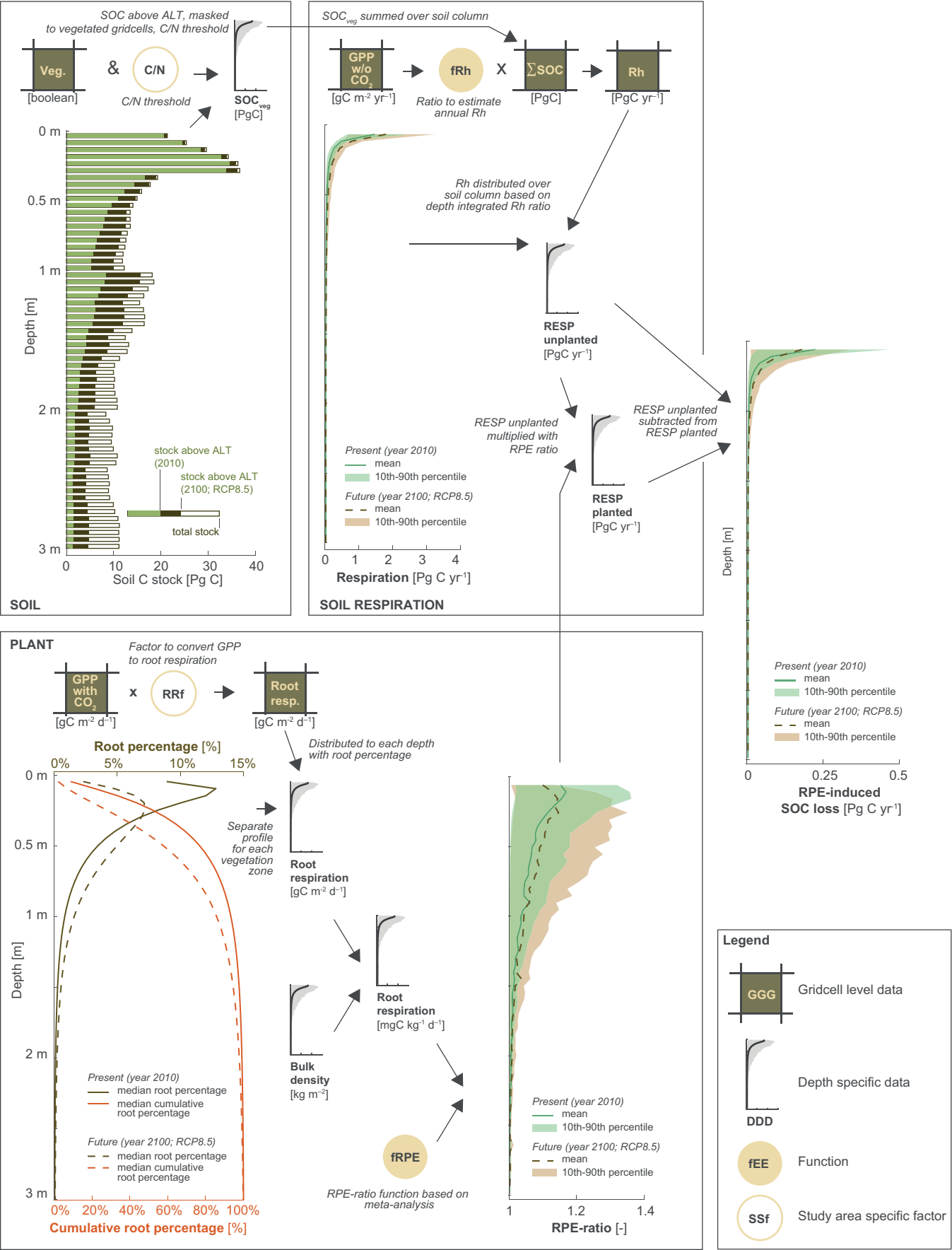
SOC above ALT, masked to vegetated gridcells, C/N threshold
Veg.
[boolean]
&
C/N
C/N threshold
SOC_veg [PgC]
0 m
0.5 m
1 m
2 m
3 m
Depth [m]
stock above ALT (2010)
stock above ALT (2100; RCP8.5)
total stock
0
10
20
30
40
Soil C stock [Pg C]
SOIL
SOC_veg summed over soil column
GPP w/o CO2
[gC m-2 yr-1]
fRh
Ratio to estimate annual Rh
X
∑SOC
[PgC]
Rh
[PgC yr-1]
Rh distributed over soil column based on depth integrated Rh ratio
RESP unplanted
[PgC yr-1]
RESP unplanted multiplied with RPE ratio
RESP planted
[PgC yr-1]
RESP unplanted subtracted from RESP planted
Present (year 2010)
mean
10th-90th percentile
Future (year 2100; RCP8.5)
mean
10th-90th percentile
0
1
2
3
4
Respiration [Pg C yr-1]
SOIL RESPIRATION
Depth [m]
Present (year 2010)
mean
10th-90th percentile
Future (year 2100; RCP8.5)
mean
10th-90th percentile
0
0.25
0.5
RPE-induced SOC loss [Pg C yr-1]
PLANT
Factor to convert GPP to root respiration
GPP with CO2
[gC m-2 d-1]
x
RRf
Root resp.
[gC m-2 d-1]
Root percentage [%]
0%
5%
10%
15%
Distributed to each depth with root percentage
Separate profile for each vegetation zone
Root respiration
[gC m-2 d-1]
Root respiration
[mgC kg-1 d-1]
Bulk density
[kg m-2]
fRPE
RPE-ratio function based on meta-analysis
Present (year 2010)
median root percentage
median cumulative root percentage
Future (year 2100; RCP8.5)
median root percentage
median cumulative root percentage
0%
20%
40%
60%
80%
100%
Cumulative root percentage [%]
Present (year 2010)
mean
10th-90th percentile
Future (year 2100; RCP8.5)
mean
10th-90th percentile
1
1.2
1.4
RPE-ratio [-]
Legend
GGG
Gridcell level data
DDD
Depth specific data
fEE
Function
SSf
Study area specific factor

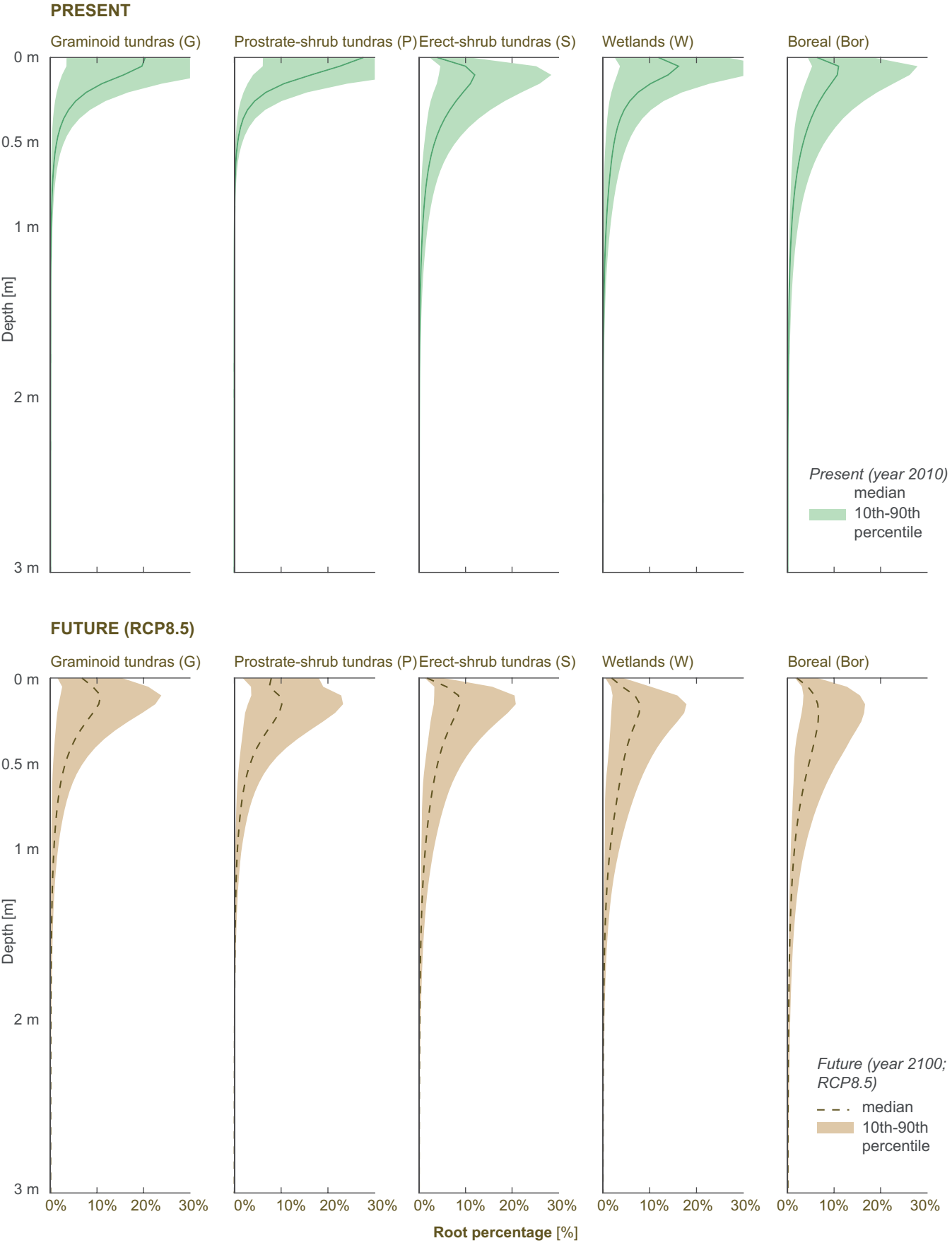
PRESENT
Graminoid tundras (G)
Prostrate-shrub tundras (P)
Erect-shrub tundras (S)
Wetlands (W)
Boreal (Bor)
0 m
0.5 m
1 m
2 m
3 m
Depth [m]
Present (year 2010)
median
10th-90th percentile
FUTURE (RCP8.5)
Graminoid tundras (G)
Prostrate-shrub tundras (P)
Erect-shrub tundras (S)
Wetlands (W)
Boreal (Bor)
0 m
0.5 m
1 m
2 m
3 m
Depth [m]
Future (year 2100; RCP8.5)
median
10th-90th percentile
0%
10%
20%
30%
Root percentage [%]

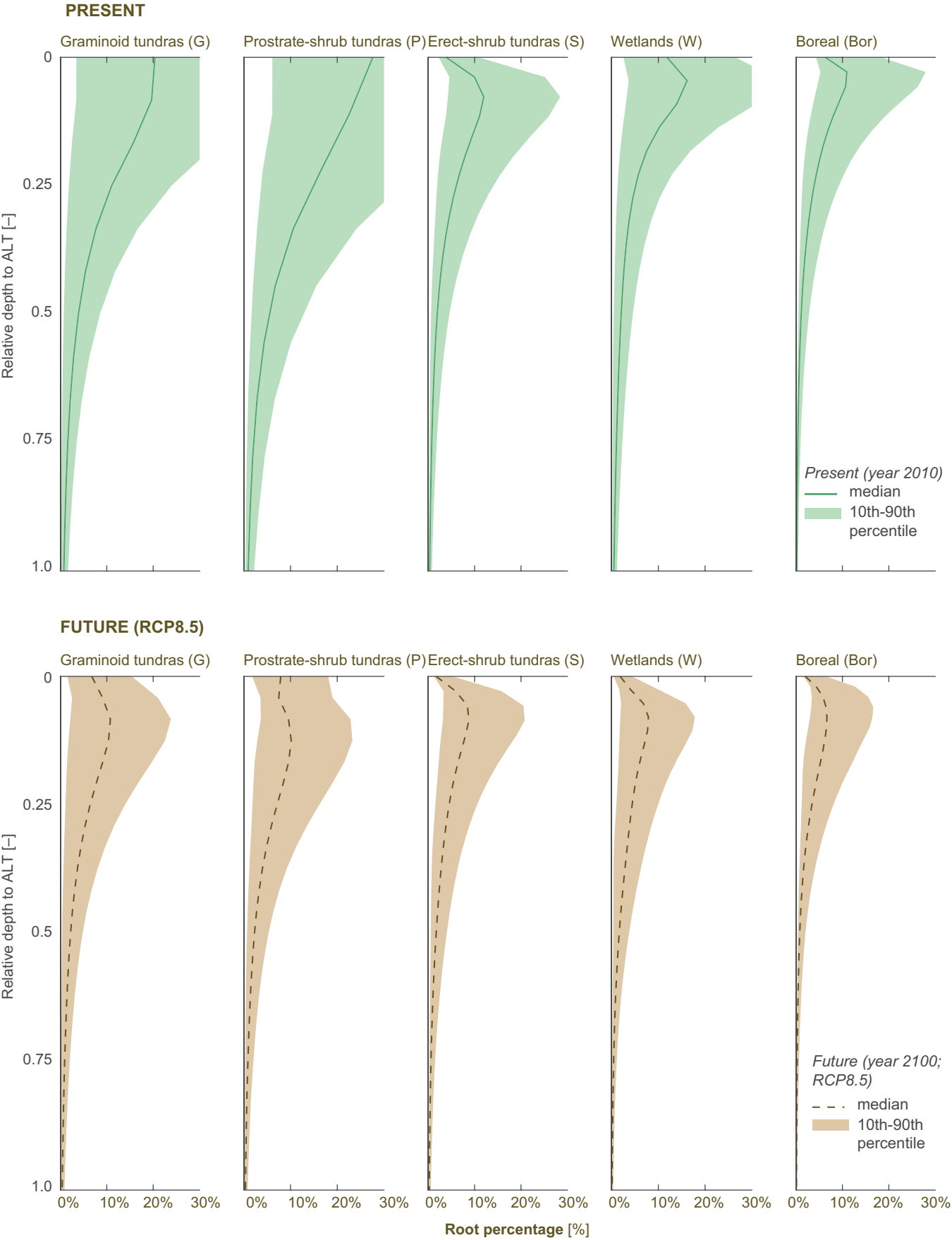
PRESENT
Graminoid tundras (G)
Prostrate-shrub tundras (P)
Erect-shrub tundras (S)
Wetlands (W)
Boreal (Bor)
Relative depth to ALT [–]
0
0.25
0.5
0.75
1.0
Present (year 2010)
median
10th-90th percentile
FUTURE (RCP8.5)
Graminoid tundras (G)
Prostrate-shrub tundras (P)
Erect-shrub tundras (S)
Wetlands (W)
Boreal (Bor)
Relative depth to ALT [–]
0
0.25
0.5
0.75
1.0
Future (year 2100; RCP8.5)
median
10th-90th percentile
0%
10%
20%
30%
Root percentage [%]

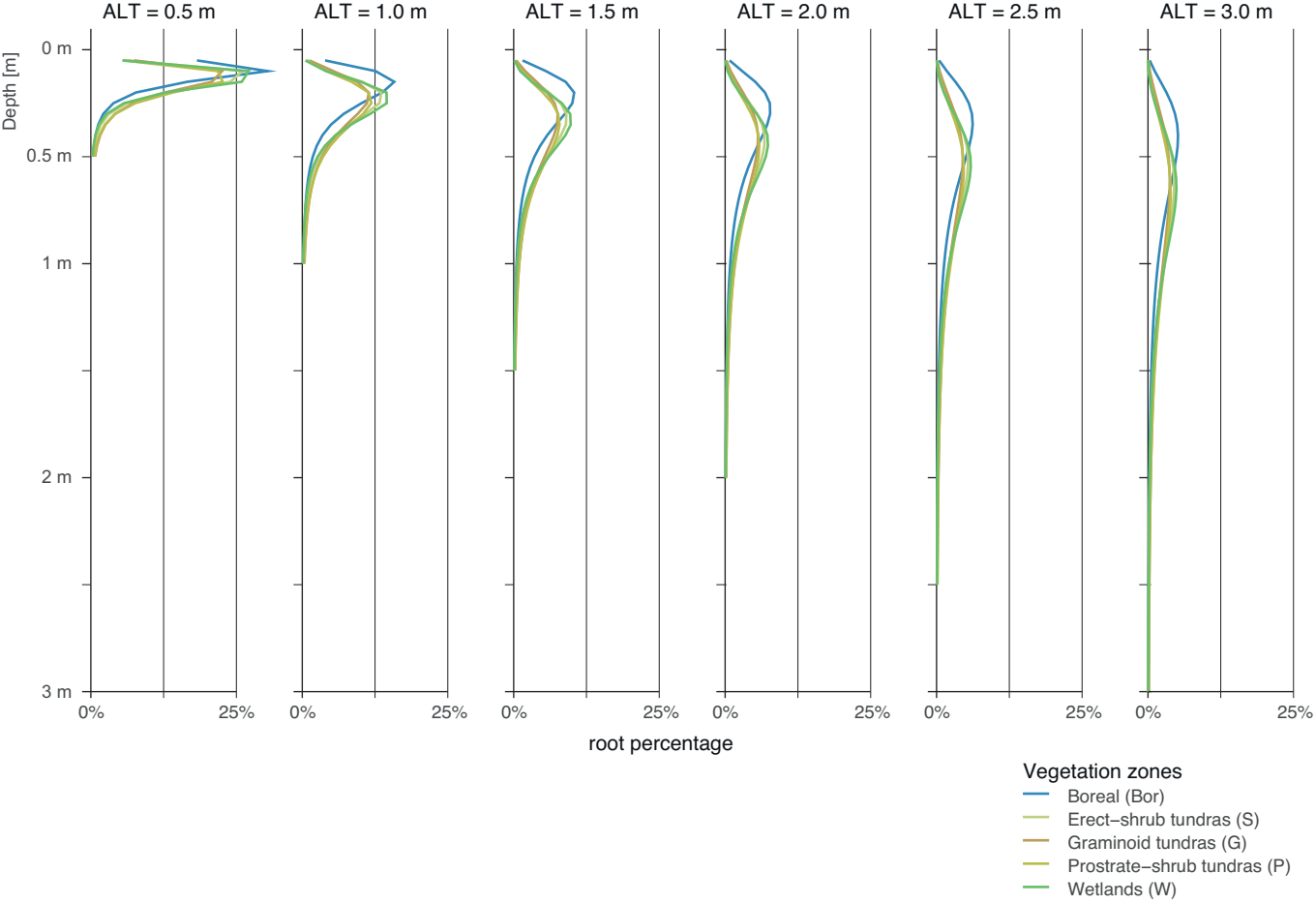
ALT = 0.5 m
ALT = 1.0 m
ALT = 1.5 m
ALT = 2.0 m
ALT = 2.5 m
ALT = 3.0 m
Depth [m]
0 m
0.5 m
1 m
2 m
3 m
0%
25%
root percentage
Vegetation zones
Boreal (Bor)
Erect−shrub tundras (S)
Graminoid tundras (G)
Prostrate−shrub tundras (P)
Wetlands (W)

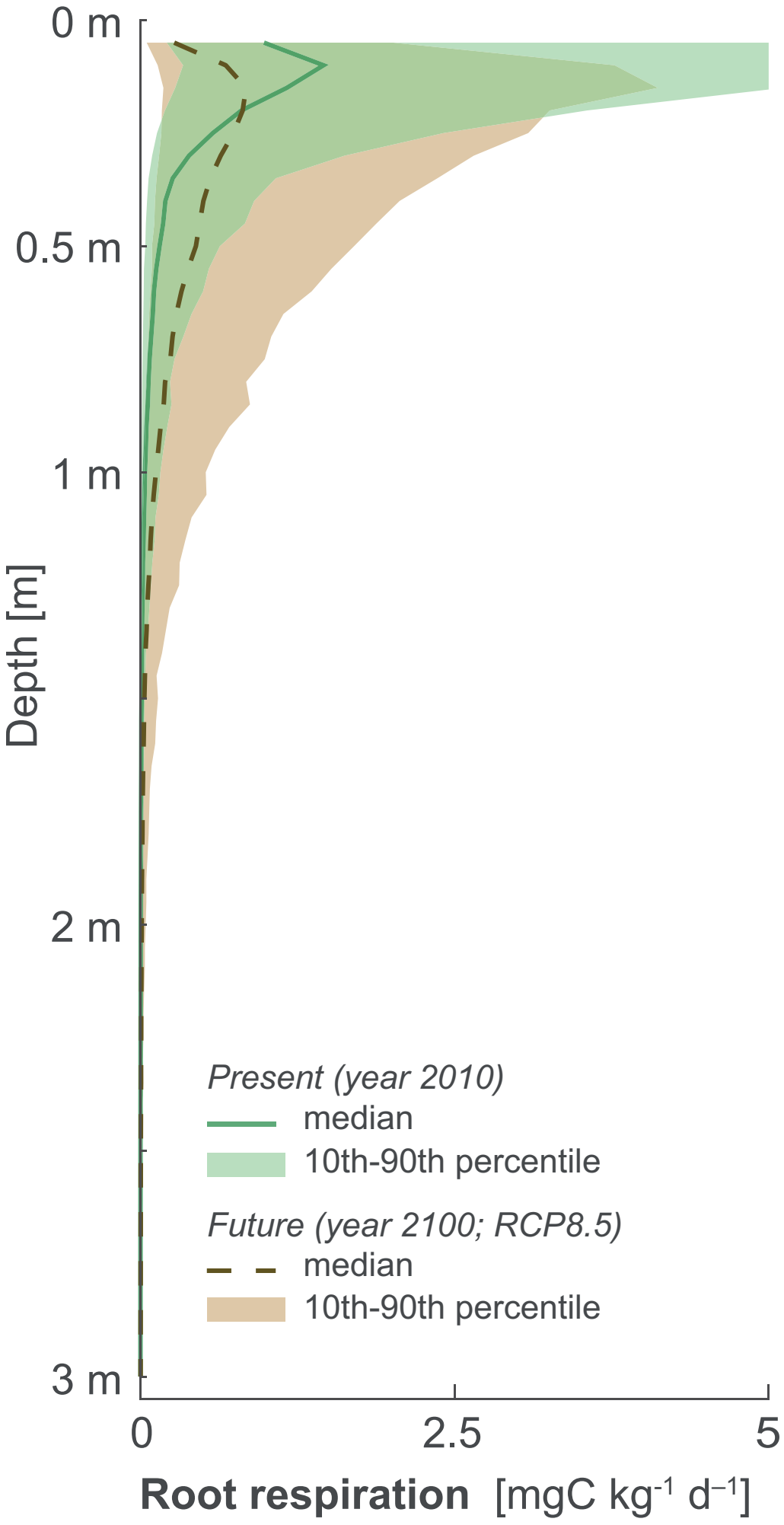
0 m
0.5 m
1 m
2 m
3 m
Depth [m]
Present (year 2010)
median
10th-90th percentile
Future (year 2100; RCP8.5)
median
10th-90th percentile
0
2.5
5
Root respiration [mgC kg-1 d-1]

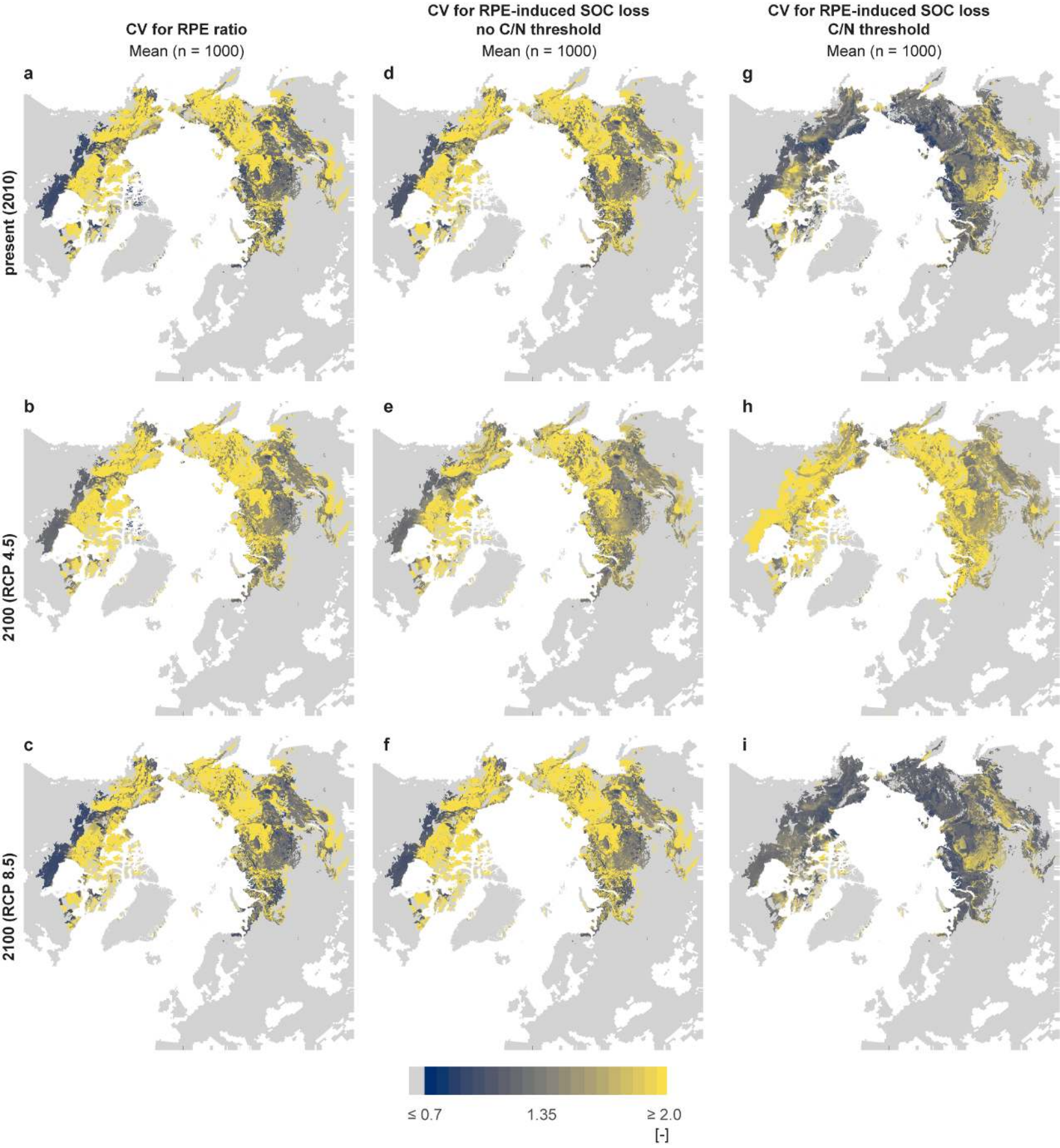
CV for RPE ratio
Mean (n = 1000)
CV for RPE-induced SOC loss
no C/N threshold
Mean (n = 1000)
CV for RPE-induced SOC loss
C/N threshold
Mean (n = 1000)
a
b
c
d
e
f
g
h
i
present (2010)
2100 (RCP 4.5)
2100 (RCP 8.5)
≤ 0.7
1.35
≥ 2.0
[-]

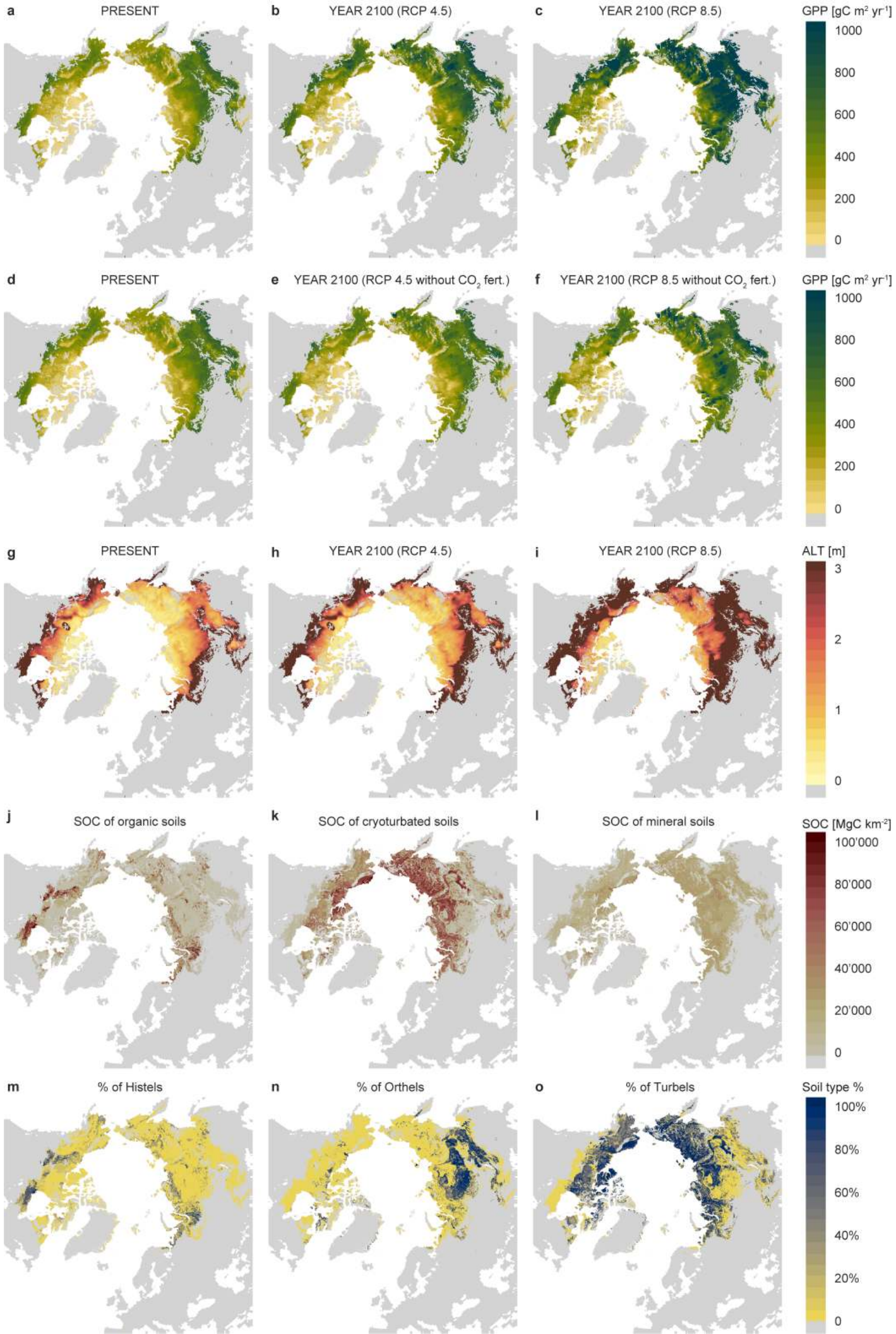
a
PRESENT
b
YEAR 2100 (RCP 4.5)
c
YEAR 2100 (RCP 8.5)
GPP [gC m² yr⁻¹]
1000
800
600
400
200
0
d
PRESENT
e
YEAR 2100 (RCP 4.5 without CO2 fert.)
f
YEAR 2100 (RCP 8.5 without CO2 fert.)
GPP [gC m² yr⁻¹]
1000
800
600
400
200
0
g
PRESENT
h
YEAR 2100 (RCP 4.5)
i
YEAR 2100 (RCP 8.5)
ALT [m]
3
2
1
0
j
SOC of organic soils
k
SOC of cryoturbated soils
l
SOC of mineral soils
SOC [MgC km⁻²]
100'000
80'000
60'000
40'000
20'000
0
m
% of Histels
n
% of Orthels
o
% of Turbels
Soil type %
100%
80%
60%
40%
20%
0

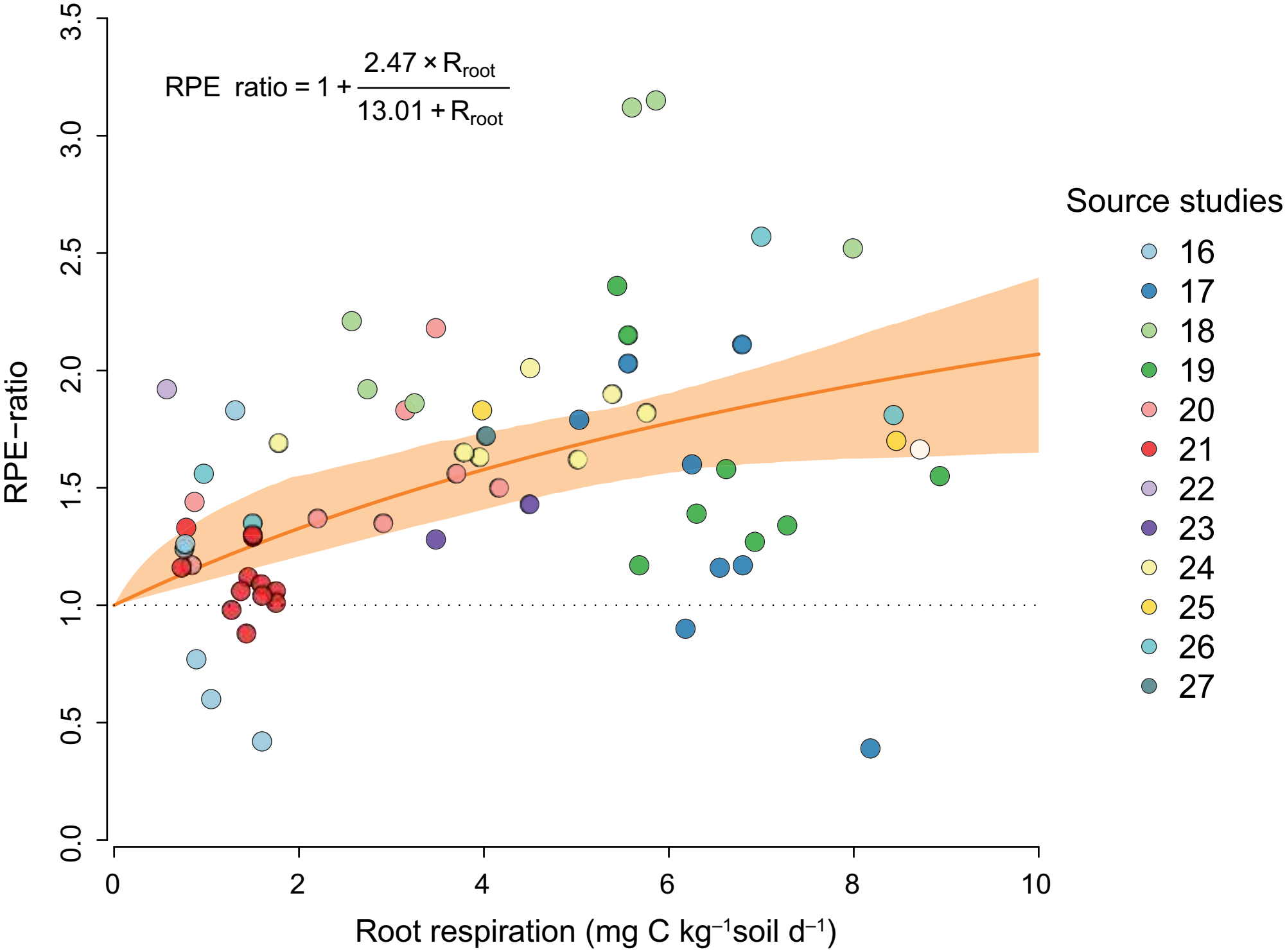
RPE ratio = 1 + 2.47 × R_root / 13.01 + R_root
RPE−ratio
0.0
0.5
1.0
1.5
2.0
2.5
3.0
3.5
0
2
4
6
8
10
Root respiration (mg C kg⁻¹soil d⁻¹)
Source studies
16
17
18
19
20
21
22
23
24
25
26
27

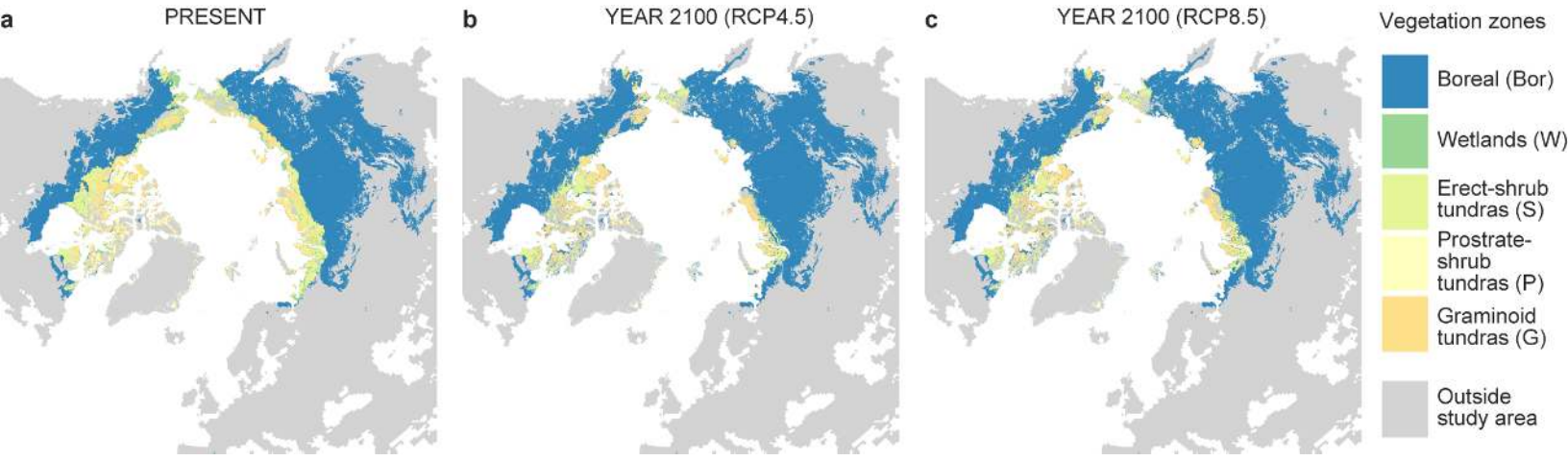
a
PRESENT
b
YEAR 2100 (RCP4.5)
c
YEAR 2100 (RCP8.5)
Vegetation zones
Boreal (Bor)
Wetlands (W)
Erect-shrub tundras (S)
Prostrate-shrub tundras (P)
Graminoid tundras (G)
Outside study area

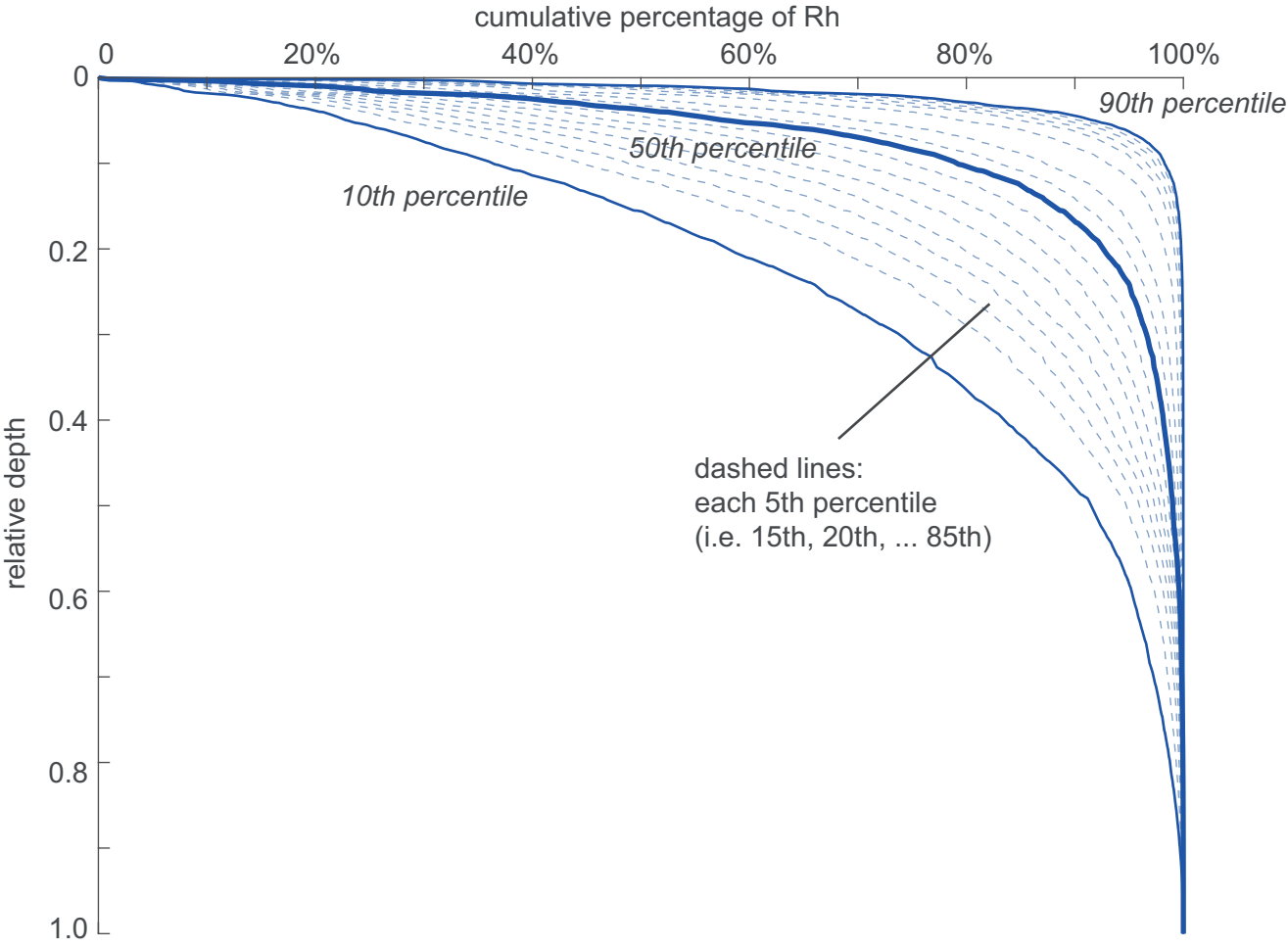
cumulative percentage of Rh
0
20%
40%
60%
80%
100%
relative depth
0
0.2
0.4
0.6
0.8
1.0
90th percentile
50th percentile
10th percentile
dashed lines:
each 5th percentile
(i.e. 15th, 20th, ... 85th)

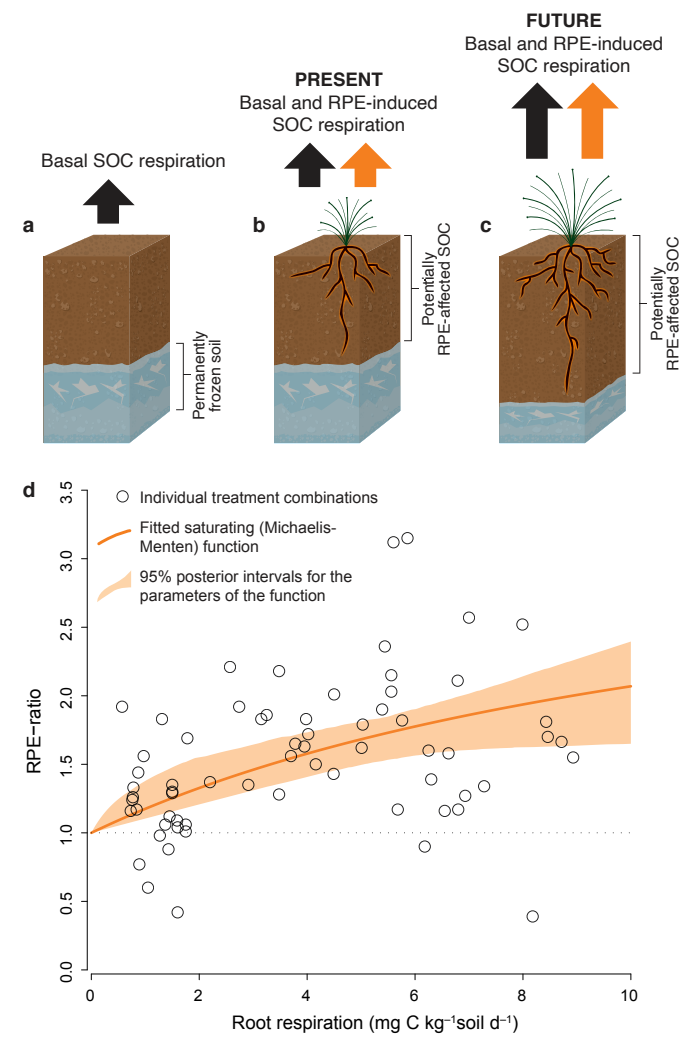
FUTURE
Basal and RPE-induced SOC respiration
PRESENT
Basal and RPE-induced SOC respiration
Basal SOC respiration
a
b
c
Permanently frozen soil
Potentially RPE-affected SOC
Potentially RPE-affected SOC
d
Individual treatment combinations
Fitted saturating (Michaelis-Menten) function
95% posterior intervals for the parameters of the function
RPE−ratio
0.0
0.5
1.0
1.5
2.0
2.5
3.0
3.5
0
2
4
6
8
10
Root respiration (mg C kg⁻¹soil d⁻¹)

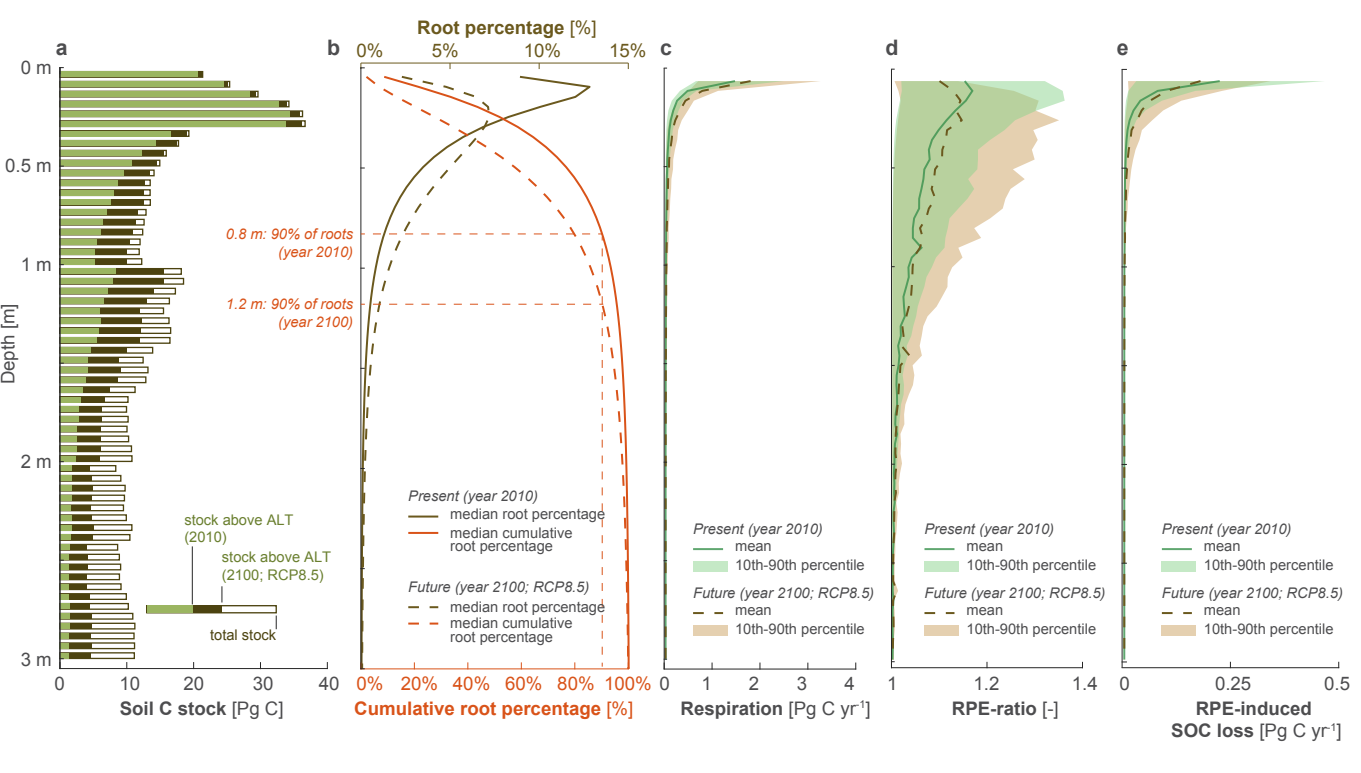
a
b
c
d
e
Root percentage [%]
0%
5%
10%
15%
0 m
0.5 m
1 m
2 m
3 m
Depth [m]
0.8 m: 90% of roots (year 2010)
1.2 m: 90% of roots (year 2100)
stock above ALT (2010)
stock above ALT (2100; RCP8.5)
total stock
Present (year 2010)
median root percentage
median cumulative root percentage
Future (year 2100; RCP8.5)
median root percentage
median cumulative root percentage
Present (year 2010)
mean
10th-90th percentile
Future (year 2100; RCP8.5)
mean
10th-90th percentile
Present (year 2010)
mean
10th-90th percentile
Future (year 2100; RCP8.5)
mean
10th-90th percentile
Present (year 2010)
mean
10th-90th percentile
Future (year 2100; RCP8.5)
mean
10th-90th percentile
0
10
20
30
40
Soil C stock [Pg C]
0%
20%
40%
60%
80%
100%
Cumulative root percentage [%]
0
1
2
3
4
Respiration [Pg C yr-1]
1
1.2
1.4
RPE-ratio [-]
0
0.25
0.5
RPE-induced SOC loss [Pg C yr-1]

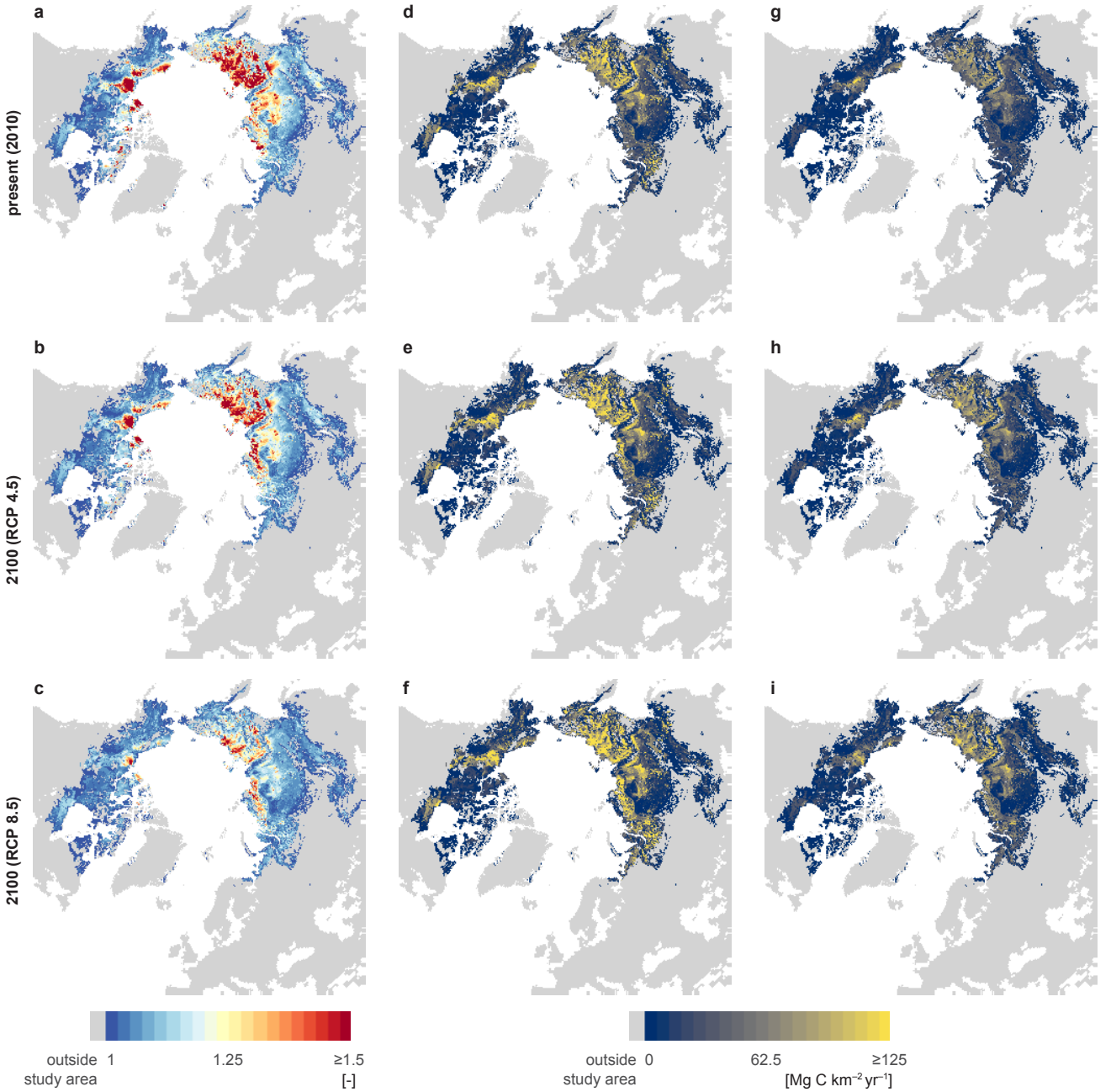
RPE ratio
Mean (n = 1000)
RPE-induced SOC loss
no C/N threshold
Mean (n = 1000)
RPE-induced SOC loss
C/N threshold
Mean (n = 1000)
a
b
c
d
e
f
g
h
i
present (2010)
2100 (RCP 4.5)
2100 (RCP 8.5)
outside study area
1
1.25
≥1.5
[-]
outside study area
0
62.5
≥125
[Mg C km−2 yr−1]

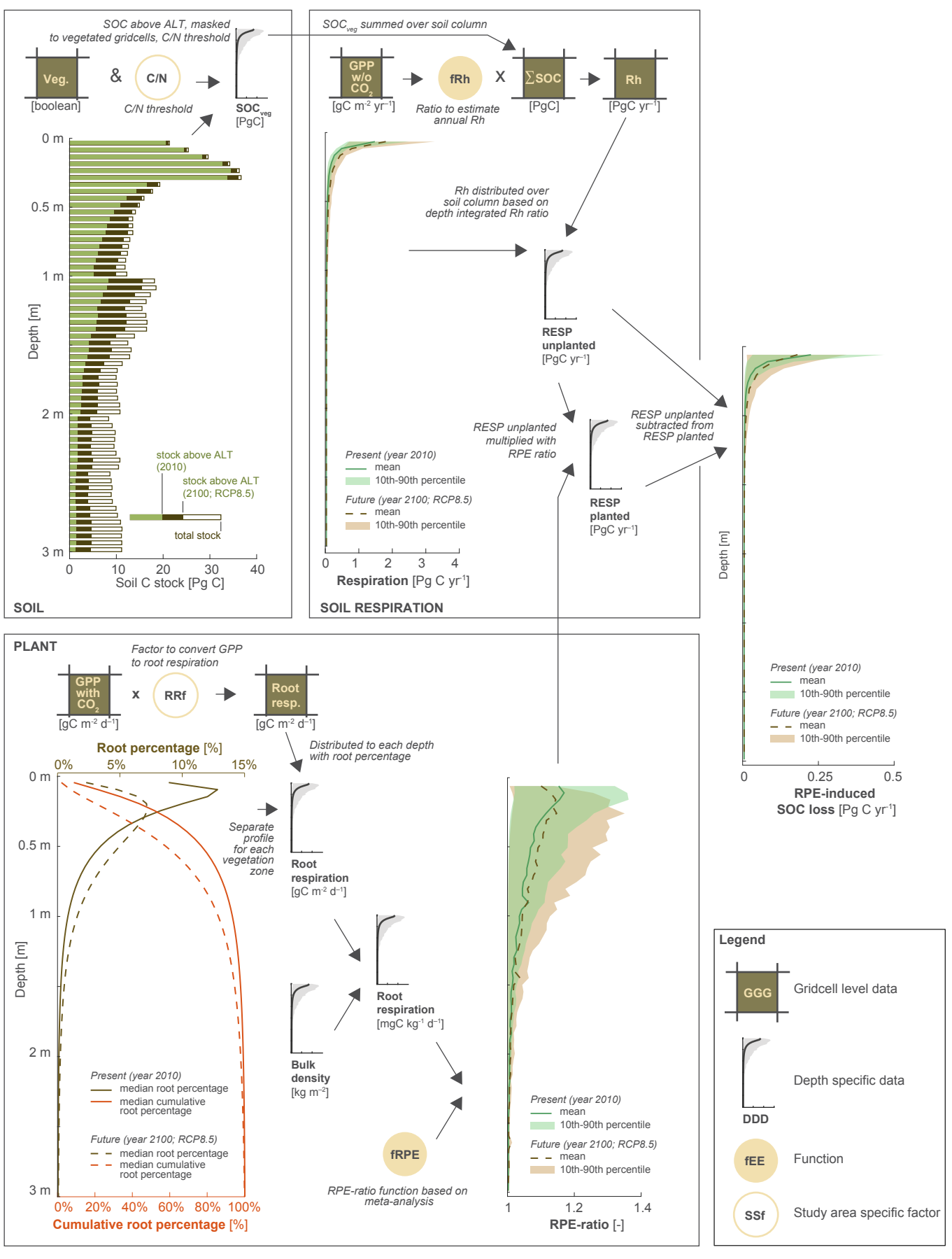
SOC above ALT, masked to vegetated gridcells, C/N threshold
Veg.
[boolean]
&
C/N
C/N threshold
SOC_veg [PgC]
0 m
0.5 m
1 m
2 m
3 m
Depth [m]
stock above ALT (2010)
stock above ALT (2100; RCP8.5)
total stock
0
10
20
30
40
Soil C stock [Pg C]
SOIL
SOC_veg summed over soil column
GPP w/o CO2
[gC m-2 yr-1]
fRh
Ratio to estimate annual Rh
X
∑SOC
[PgC]
Rh
[PgC yr-1]
Rh distributed over soil column based on depth integrated Rh ratio
RESP unplanted
[PgC yr-1]
RESP unplanted multiplied with RPE ratio
RESP planted
[PgC yr-1]
RESP unplanted subtracted from RESP planted
Present (year 2010)
mean
10th-90th percentile
Future (year 2100; RCP8.5)
mean
10th-90th percentile
0
1
2
3
4
Respiration [Pg C yr-1]
SOIL RESPIRATION
Depth [m]
Present (year 2010)
mean
10th-90th percentile
Future (year 2100; RCP8.5)
mean
10th-90th percentile
0
0.25
0.5
RPE-induced SOC loss [Pg C yr-1]
PLANT
Factor to convert GPP to root respiration
GPP with CO2
[gC m-2 d-1]
x
RRf
Root resp.
[gC m-2 d-1]
Distributed to each depth with root percentage
Root percentage [%]
0%
5%
10%
15%
0 m
0.5 m
1 m
2 m
3 m
Depth [m]
Separate profile for each vegetation zone
Root respiration
[gC m-2 d-1]
Root respiration
[mgC kg-1 d-1]
Bulk density
[kg m-2]
fRPE
RPE-ratio function based on meta-analysis
Present (year 2010)
median root percentage
median cumulative root percentage
Future (year 2100; RCP8.5)
median root percentage
median cumulative root percentage
0%
20%
40%
60%
80%
100%
Cumulative root percentage [%]
Present (year 2010)
mean
10th-90th percentile
Future (year 2100; RCP8.5)
mean
10th-90th percentile
1
1.2
1.4
RPE-ratio [-]
Legend
GGG
Gridcell level data
DDD
Depth specific data
fEE
Function
SSf
Study area specific factor

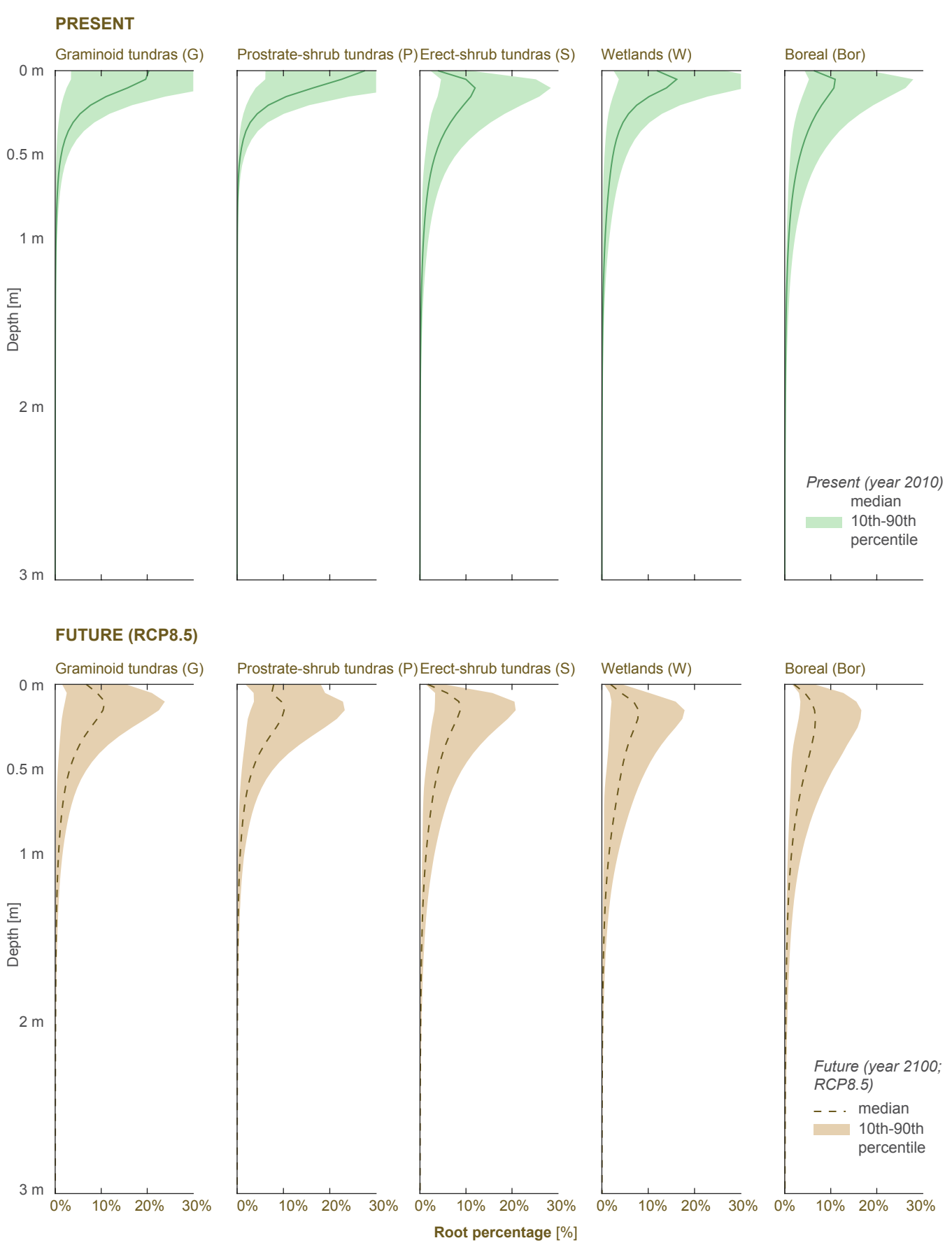
PRESENT
Graminoid tundras (G)
Prostrate-shrub tundras (P)
Erect-shrub tundras (S)
Wetlands (W)
Boreal (Bor)
0 m
0.5 m
1 m
2 m
3 m
Depth [m]
Present (year 2010)
median
10th-90th percentile
FUTURE (RCP8.5)
Graminoid tundras (G)
Prostrate-shrub tundras (P)
Erect-shrub tundras (S)
Wetlands (W)
Boreal (Bor)
0 m
0.5 m
1 m
2 m
3 m
Depth [m]
Future (year 2100; RCP8.5)
median
10th-90th percentile
0%
10%
20%
30%
Root percentage [%]

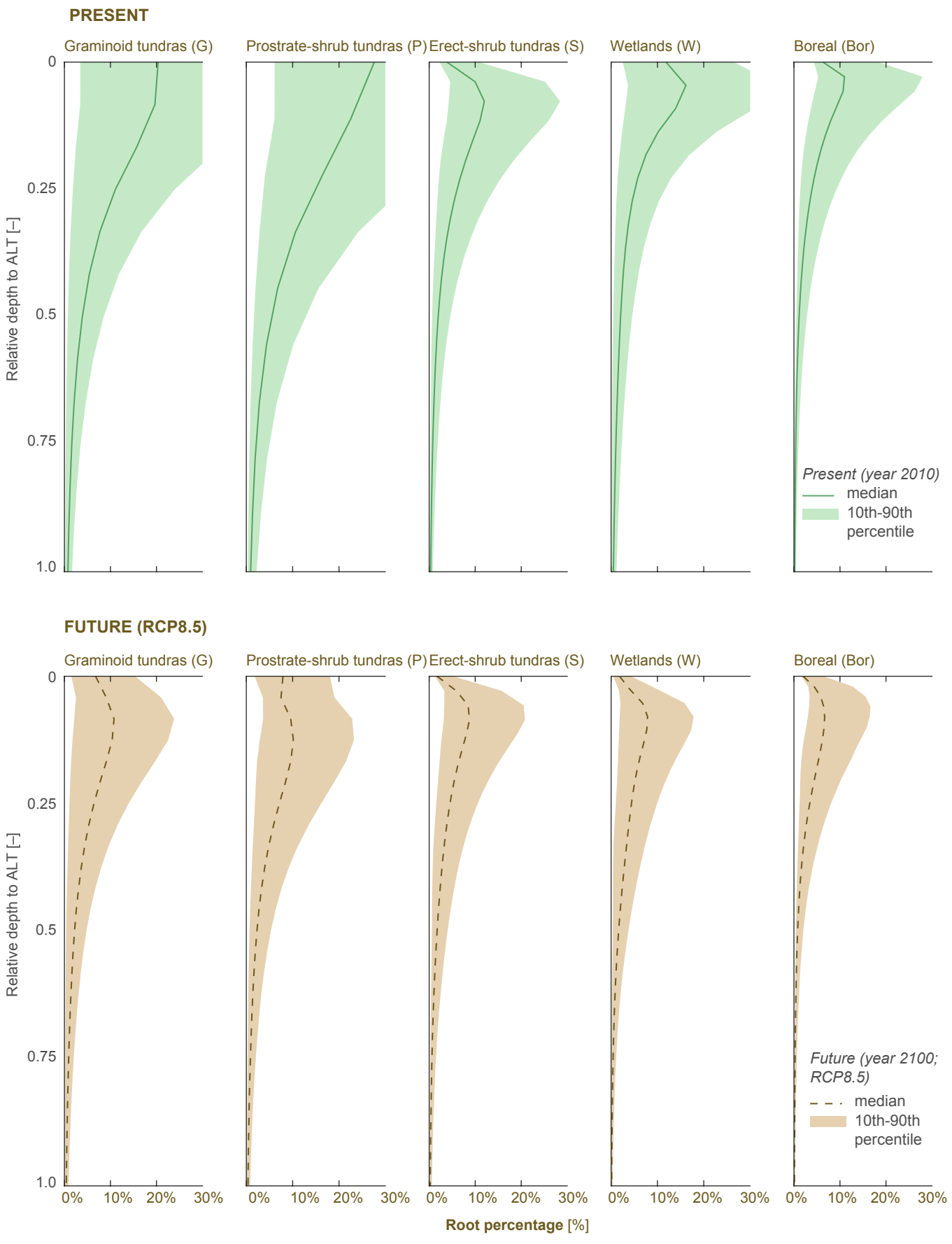
PRESENT
Graminoid tundras (G)
Prostrate-shrub tundras (P)
Erect-shrub tundras (S)
Wetlands (W)
Boreal (Bor)
Relative depth to ALT [–]
0
0.25
0.5
0.75
1.0
Present (year 2010)
median
10th-90th percentile
FUTURE (RCP8.5)
Graminoid tundras (G)
Prostrate-shrub tundras (P)
Erect-shrub tundras (S)
Wetlands (W)
Boreal (Bor)
Relative depth to ALT [–]
0
0.25
0.5
0.75
1.0
Future (year 2100; RCP8.5)
median
10th-90th percentile
0%
10%
20%
30%
Root percentage [%]

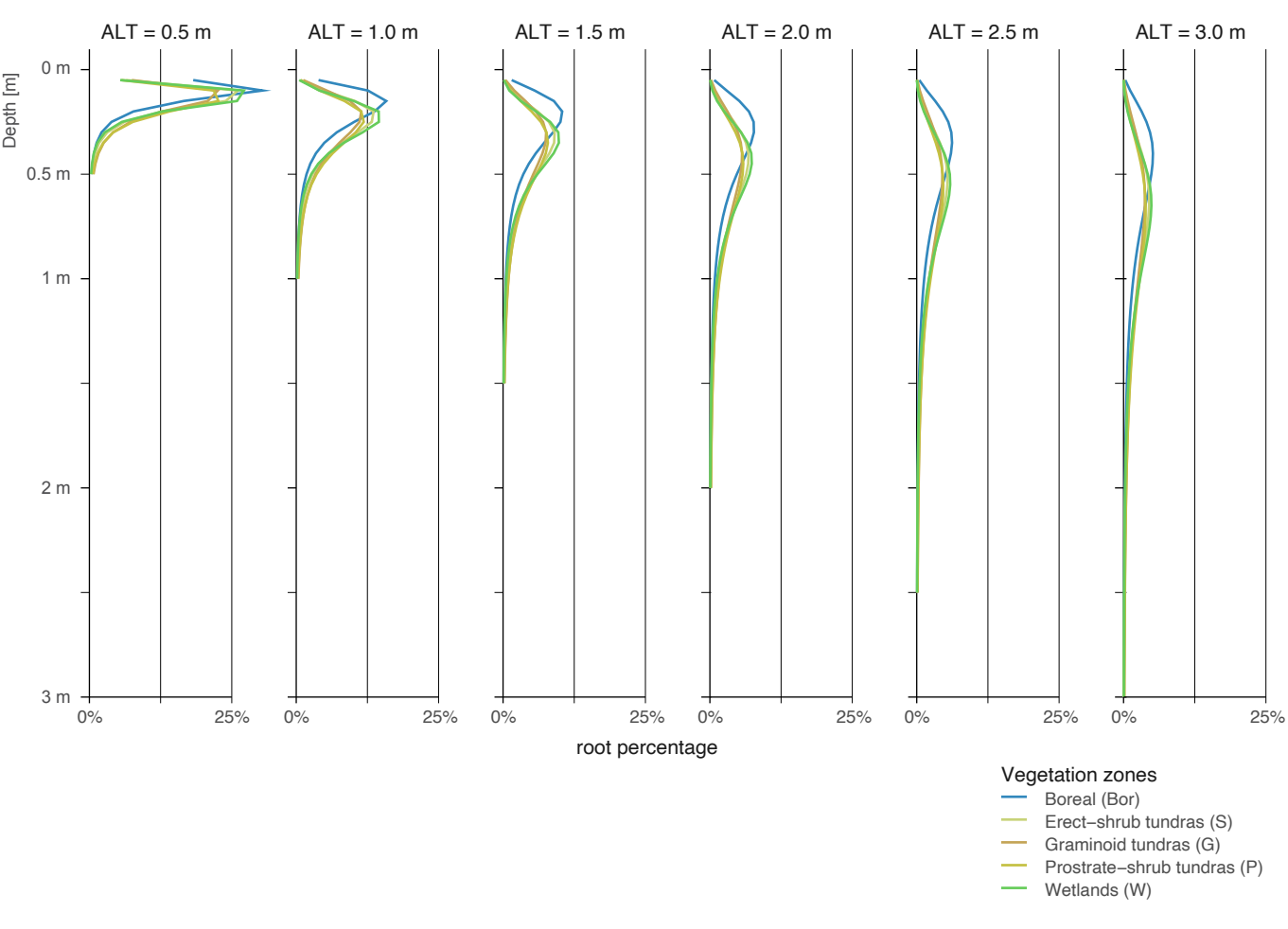
ALT = 0.5 m
ALT = 1.0 m
ALT = 1.5 m
ALT = 2.0 m
ALT = 2.5 m
ALT = 3.0 m
Depth [m]
0 m
0.5 m
1 m
2 m
3 m
0%
25%
root percentage
Vegetation zones
Boreal (Bor)
Erect−shrub tundras (S)
Graminoid tundras (G)
Prostrate−shrub tundras (P)
Wetlands (W)

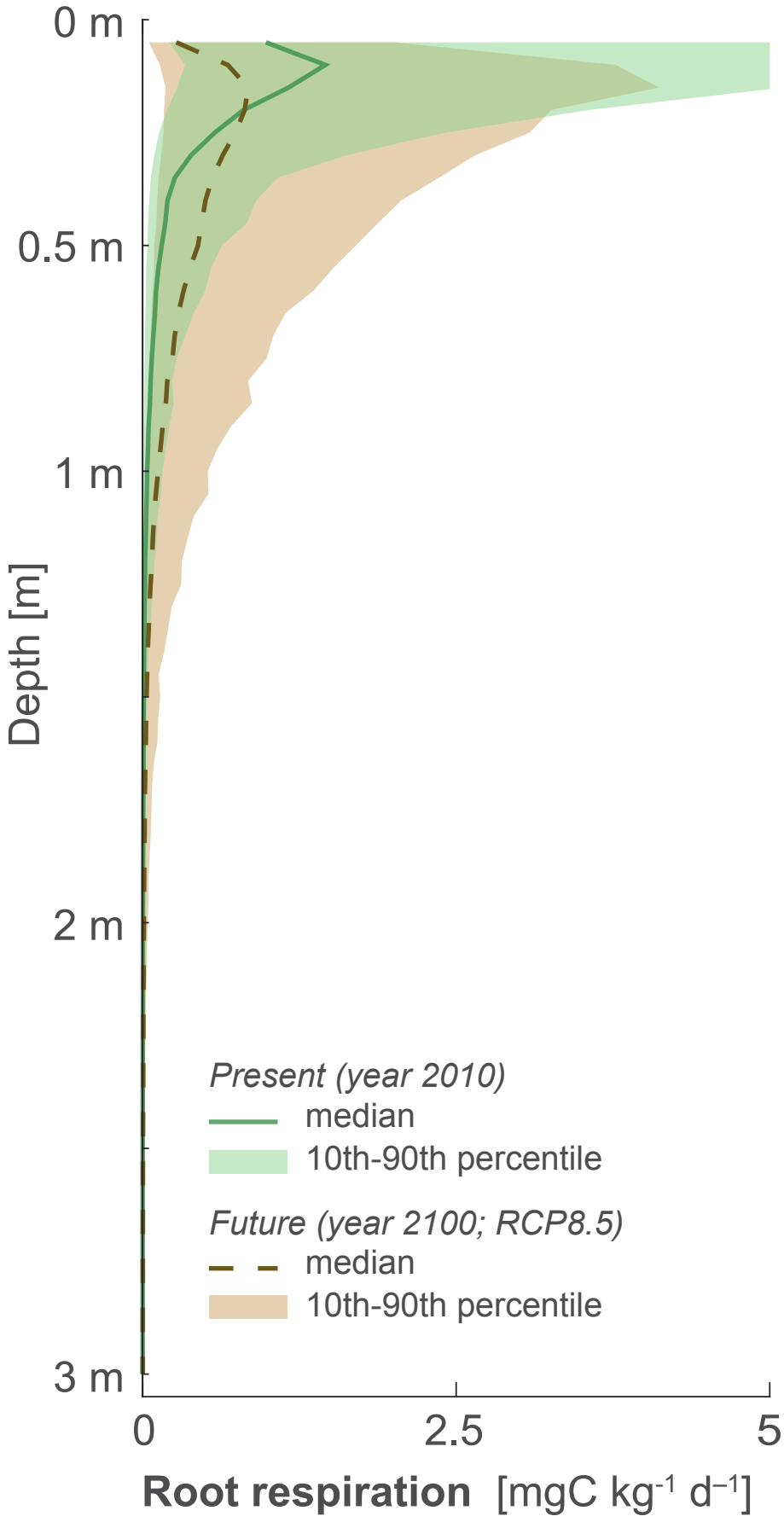
0 m
0.5 m
1 m
2 m
3 m
Depth [m]
Present (year 2010)
median
10th-90th percentile
Future (year 2100; RCP8.5)
median
10th-90th percentile
0
2.5
5
Root respiration [mgC kg-1 d-1]

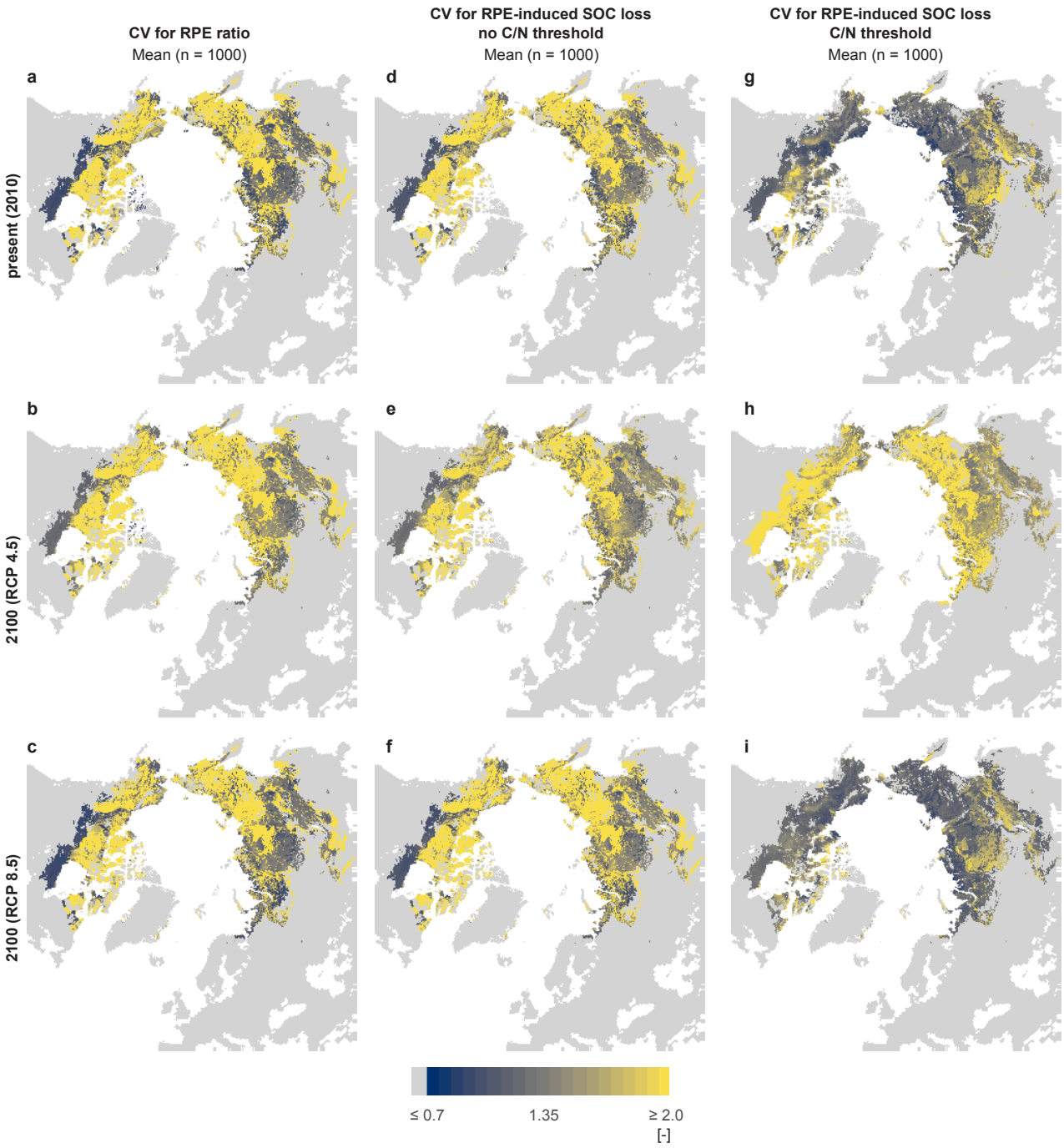
CV for RPE ratio
Mean (n = 1000)
CV for RPE-induced SOC loss
no C/N threshold
Mean (n = 1000)
CV for RPE-induced SOC loss
C/N threshold
Mean (n = 1000)
a
b
c
d
e
f
g
h
i
present (2010)
2100 (RCP 4.5)
2100 (RCP 8.5)
≤ 0.7
1.35
≥ 2.0
[-]

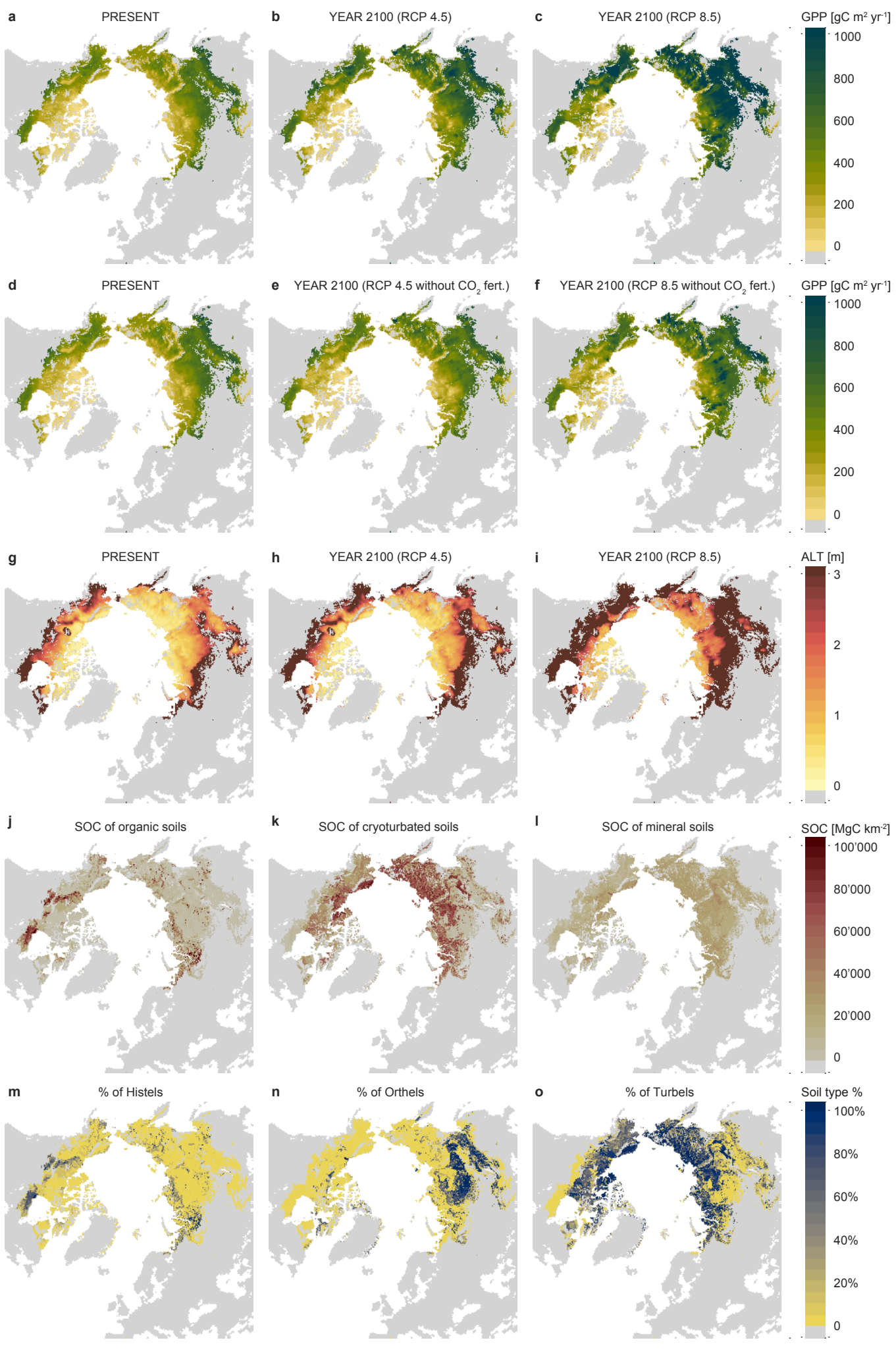
a
PRESENT
b
YEAR 2100 (RCP 4.5)
c
YEAR 2100 (RCP 8.5)
GPP [gC m² yr⁻¹]
1000
800
600
400
200
0
d
PRESENT
e
YEAR 2100 (RCP 4.5 without CO2 fert.)
f
YEAR 2100 (RCP 8.5 without CO2 fert.)
GPP [gC m² yr⁻¹]
1000
800
600
400
200
0
g
PRESENT
h
YEAR 2100 (RCP 4.5)
i
YEAR 2100 (RCP 8.5)
ALT [m]
3
2
1
0
j
SOC of organic soils
k
SOC of cryoturbated soils
l
SOC of mineral soils
SOC [MgC km⁻²]
100'000
80'000
60'000
40'000
20'000
0
m
% of Histels
n
% of Orthels
o
% of Turbels
Soil type %
100%
80%
60%
40%
20%
0

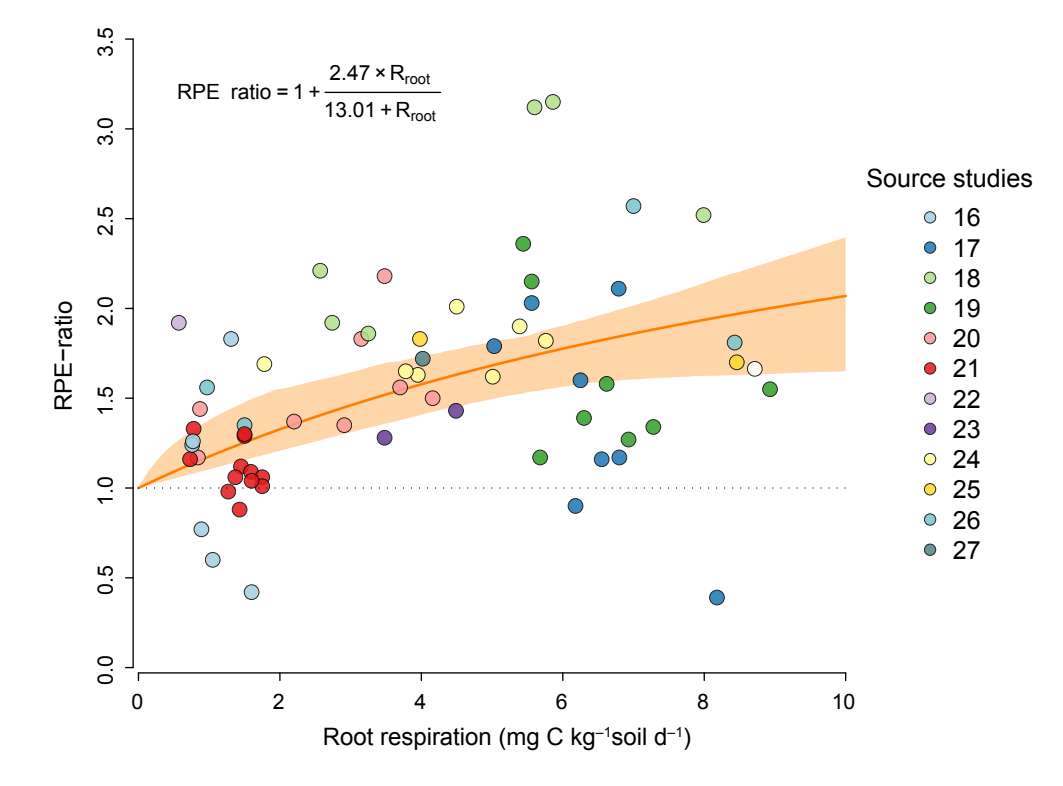
RPE ratio = 1 + 2.47 × R_root / 13.01 + R_root
RPE−ratio
0.0
0.5
1.0
1.5
2.0
2.5
3.0
3.5
0
2
4
6
8
10
Root respiration (mg C kg⁻¹soil d⁻¹)
Source studies
16
17
18
19
20
21
22
23
24
25
26
27

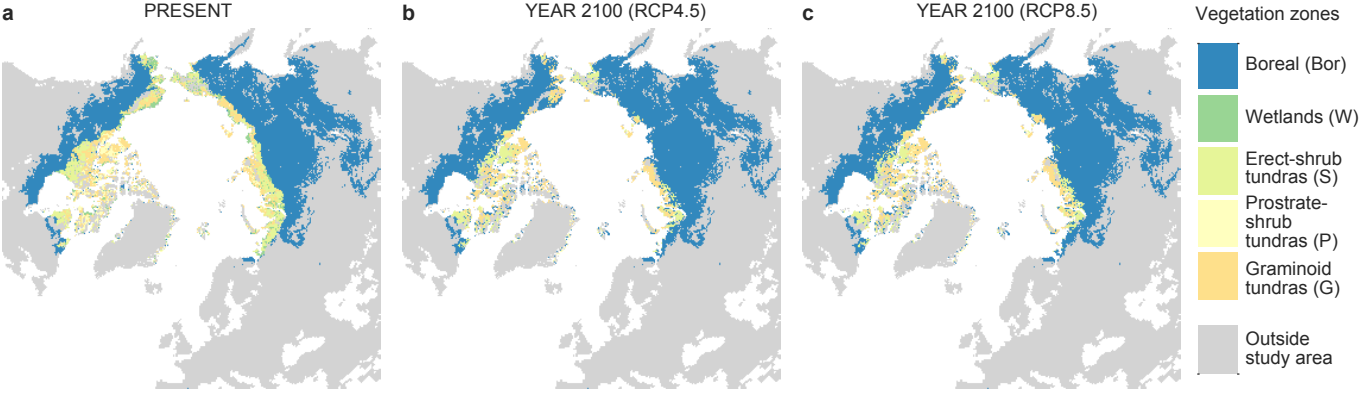
a
PRESENT
b
YEAR 2100 (RCP4.5)
c
YEAR 2100 (RCP8.5)
Vegetation zones
Boreal (Bor)
Wetlands (W)
Erect-shrub tundras (S)
Prostrate-shrub tundras (P)
Graminoid tundras (G)
Outside study area

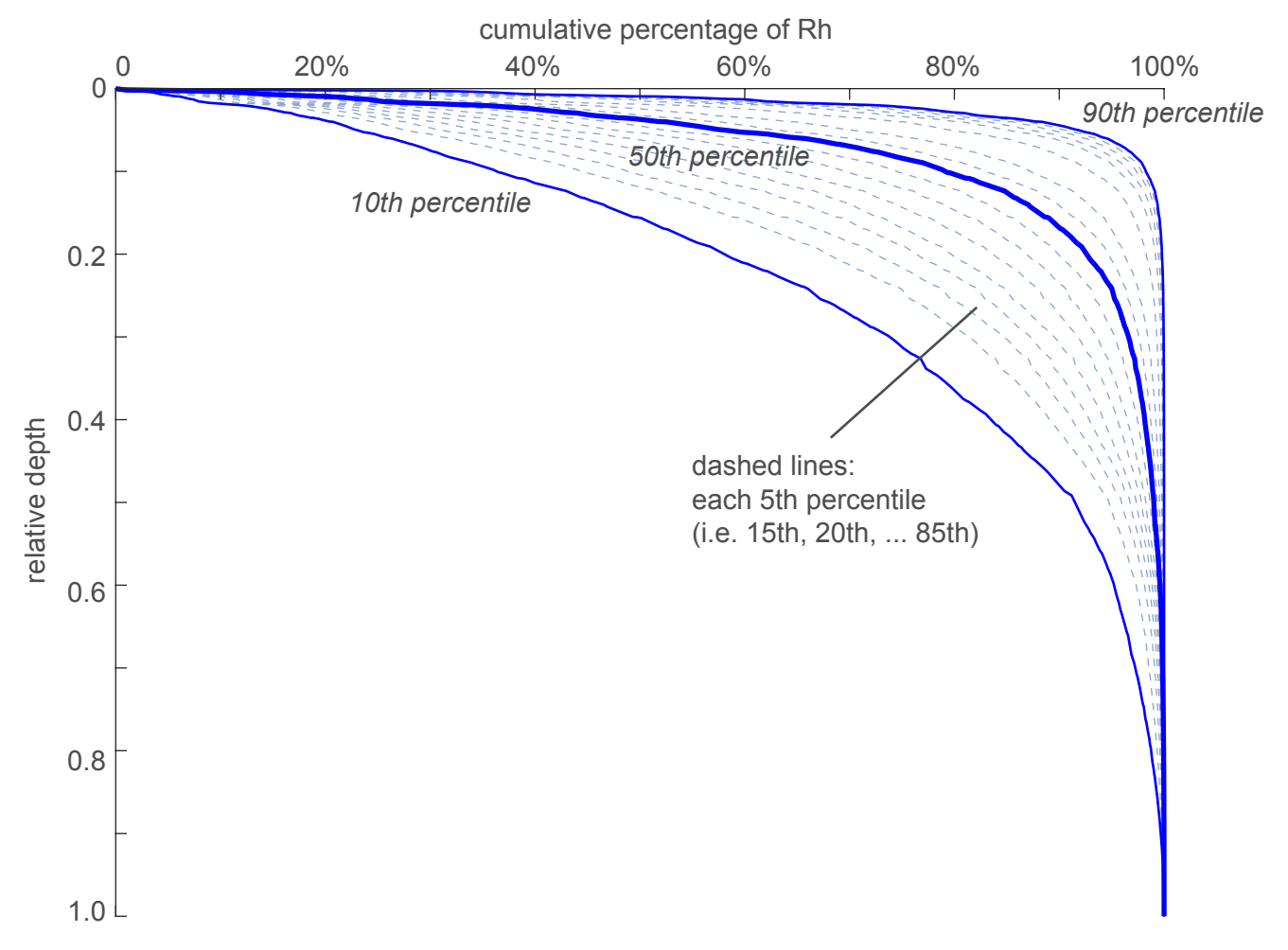
cumulative percentage of Rh
0
20%
40%
60%
80%
100%
relative depth
0
0.2
0.4
0.6
0.8
1.0
90th percentile
50th percentile
10th percentile
dashed lines:
each 5th percentile
(i.e. 15th, 20th, ... 85th)